Title

Siddhartha Patra,[1] Abhirup Mukherjee,[1,*] Anirban Mukherjee,[1,†] and Siddhartha Lal[1,‡]

[1] *Department of Physical Sciences, Indian Institute of Science Education and Research-Kolkata, W.B. 741246, India*

(Dated: December 27, 2021)

Lorem ipsum dolor sit amet, consectetuer adipiscing elit. Ut purus elit, vestibulum ut, placerat ac, adipiscing vitae, felis. Curabitur dictum gravida mauris. Nam arcu libero, nonummy eget, consectetuer id, vulputate a, magna. Donec vehicula augue eu neque. Pellentesque habitant morbi tristique senectus et netus et malesuada fames ac turpis egestas. Mauris ut leo. Cras viverra metus rhoncus sem. Nulla et lectus vestibulum urna fringilla ultrices. Phasellus eu tellus sit amet tortor gravida placerat. Integer sapien est, iaculis in, pretium quis, viverra ac, nunc. Praesent eget sem vel leo ultrices bibendum. Aenean faucibus. Morbi dolor nulla, malesuada eu, pulvinar at, mollis ac, nulla. Curabitur auctor semper nulla. Donec varius orci eget risus. Duis nibh mi, congue eu, accumsan eleifend, sagittis quis, diam. Duis eget orci sit amet orci dignissim rutrum.

Nam dui ligula, fringilla a, euismod sodales, sollicitudin vel, wisi. Morbi auctor lorem non justo. Nam lacus libero, pretium at, lobortis vitae, ultricies et, tellus. Donec aliquet, tortor sed accumsan bibendum, erat ligula aliquet magna, vitae ornare odio metus a mi. Morbi ac orci et nisl hendrerit mollis. Suspendisse ut massa. Cras nec ante. Pellentesque a nulla. Cum sociis natoque penatibus et magnis dis parturient montes, nascetur ridiculus mus. Aliquam tincidunt urna. Nulla ullamcorper vestibulum turpis. Pellentesque cursus luctus mauris.

CONTENTS

* am18ip014@iiserkol.ac.in
† mukherjee.anirban.anirban@gmail.com
‡ slal@iiserkol.ac.in

I. INTRODUCTION

II. FIXED POINT THEORY OF OVER-SCREENED MCK MODEL

A. RG flows towards intermediate coupling

We start with the usual K-channel Kondo model Hamiltonian with isotropic couplings [1]:

$$H = \sum_{l=1}^{K} H_l \ ,$$
$$H_l = \sum_{k} \sum_{\alpha=\uparrow,\downarrow} \epsilon_{k,l} \hat{n}_{k\alpha,l} + J \sum_{kk'} \sum_{\alpha,\beta=\uparrow,\downarrow} \vec{S}_d \cdot \frac{1}{2} \vec{\sigma}_{\alpha\alpha'} c^{\dagger}_{k\alpha,l} c_{k'\alpha',l} \ . \tag{1}$$

Here, l sums over the K channels of the conduction bath, k, k' sum over all the momentum states of the bath and α, β sum over the two spin indices of a single electron. $c_{k\alpha,l}$ is the fermionic field operator at momentum k, spin α and channel l. $\epsilon_{k,l}$ represents the dispersion of the l^{th} conduction channel. $\vec{\sigma}$ is the vector of Pauli matrices and $\vec{S}_d = \frac{1}{2}\vec{\sigma}_d$ is the impurity spin operator.

We have performed a renormalisation group analysis of the Hamiltonian using the recently developed URG method [2–7]. The RG proceeds *by applying unitary transformations in order to block-diagonalize the Hamiltonian by removing number fluctuations of the high energy degrees of freedom.* If the most energetic electronic state at the j^{th} RG step is $|j\rangle$ defined by the energy $D_{(j)}$, the Hamiltonian will in general not conserve the number of particles in this state: $\left[H_{(j)}, \hat{n}_j\right] \neq 0$. The unitary transformation $U_{(j)}$ will remove this number fluctuation at the next RG step:

$$H_{(j-1)} = U_{(j)} H_{(j)} U^{\dagger}_{(j)}, \ \ \left[H_{(j-1)}, \hat{n}_j\right] = 0 \tag{2}$$

The unitary transformations are given in terms of a fermionic generator $\eta_{(j)}$:

$$U_{(j)} = \frac{1}{\sqrt{2}} \left(1 + \eta_{(j)} - \eta^{\dagger}_{(j)}\right), \quad \left\{\eta_{(j)}, \eta^{\dagger}_{(j)}\right\}_{\pm} = 1 \tag{3}$$

where $\{A, B\}_{\pm} = AB \pm BA$. The generator itself is given by the expression

$$\eta^{\dagger}_{(j)} = \frac{1}{\hat{\omega}_{(j)} - \text{Tr}\left(H_{(j)} \hat{n}_j\right)} c^{\dagger}_j \text{Tr}\left(H_{(j)} c_j\right) \tag{4}$$

The operator $\hat{\omega}_{(j)}$ encodes the quantum fluctuation scales arising from the interplay of the kinetic energy terms and the interaction terms of the Hamiltonian:

$$\hat{\omega}_{(j)} = H_{(j-1)} - H^{i}_{(j)} \tag{5}$$

$H^{i}_{(j)}$ is that part of $H_{(j)}$ that commutes with $\hat{n}_j$ but does not commute with at least one $\hat{n}_l$ for $l < j$. The RG continues up to energy D^* where a fixed point is reached from the vanishing of either the numerator or the denominator.

The derivation of the RG equation for the over-screened regime ($2S < K$) of the spin-S-impurity K-channel Kondo problem is shown in appendix A. On decoupling circular isoenergetic shells at energies $D_{(j)}$, the change in the Kondo coupling at the j^{th} RG step, $\Delta J_{(j)}$, is given by

$$\Delta J_{(j)} = -\frac{J^2_{(j)} \mathcal{N}_{(j)}}{\omega_{(j)} - \frac{D_{(j)}}{2} + \frac{J_{(j)}}{4}} \left(1 - \frac{1}{2} \rho J_{(j)} K\right) \tag{6}$$

$\mathcal{N}_{(j)}$ is the number of electronic states at the energy shell $D_{(j)}$. We work in the low quantum fluctuation regime $\omega_{(j)} < \frac{D_{(j)}}{2}$. There are three fixed points of the RG equation. One arises from the vanishing of the denominator, and was present in the single-channel Kondo RG equation as well [8]. As shown there, this fixed-point goes to $J^* = \infty$ as the bare bandwidth of the conduction electrons is made large. The other trivial fixed point is the trivial one at $J^* = 0$. The third fixed point is reached when the numerator vanishes: $J^* = \frac{2}{K\rho}$ [1, 9–11]. Only the intermediate fixed point is found to be stable. This is consistent with results from Bethe ansatz calculations [12–17], CFT calculations [18–20], bosonization treatments [21, 22] and NRG analysis [23, 24].

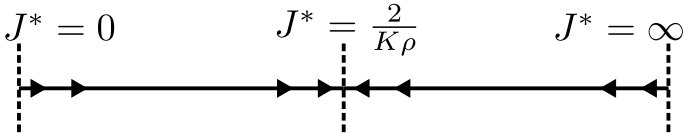

FIG. 1. The three fixed points of the over-screened RG equation. Only the intermediate one is stable.

The RG equation reduces to the perturbative form $\Delta J_{(j)} \simeq \frac{J^2_{(j)} \mathcal{N}_{(j)}}{D_{(j)}} \left(1 - \frac{1}{2} \rho J_{(j)} K\right)$ [1, 10, 11, 25] when one replaces $\omega_{(j)}$ with the ground state energy $-\frac{D_{(j)}}{2}$ and assumes $J \ll D_{(j)}$.

B. Star graph as the effective fixed point Hamiltonian

The fixed point Hamiltonian takes the form

$$H^* = \sum_{l} \left[\sum_{k}^{*} \epsilon_{k,l} \hat{n}_{k\alpha,l} + J \sum_{kk'}^{*} \vec{S}_d \cdot \frac{1}{2} \vec{\sigma}_{\alpha\alpha'} c^{\dagger}_{k\alpha,l} c_{k'\alpha',l} \ . \right] \tag{7}$$

We have not explicitly written the decoupled degrees of freedom $D_{(j)} > D^*$ in the Hamiltonian. The $*$ over the summations indicate that only the momenta inside the

window D^* enter the summation. There is an implied summation over the spin indices α, β.

To study the low energy physics and universality of the problem, we will mostly focus on the zero bandwidth limit of the fixed point Hamiltonian. Upon setting the chemical potential equal to the Fermi energy, this zero bandwidth model becomes a Heisenberg spin-exchange Hamiltonian.

$$H^* = J \sum_l \sum_{kk'}^{*} \vec{S}_d \cdot \frac{1}{2} \vec{\sigma}_{\alpha\alpha'} c^\dagger_{k\alpha,l} c_{k'\alpha',l} = J \vec{S}_d \cdot \sum_l \vec{s}_l \ . \tag{8}$$

At the last step, we defined the local spin operator $\vec{s}_l = \frac{1}{2}\sigma_l = \frac{1}{2}\sum_{kk'}^{*} \sum_{\alpha\beta} \vec{\sigma}_{\alpha\alpha'} c^\dagger_{k\alpha,l} c_{k'\alpha',l}$ of each conduction channel. The star graph commutes with several operators, including the total spin operator $J^z = S^z_d + \sum_l s^z_l$ along z, the total bath local spin operator $s^2_{\rm tot} = (\sum_l \vec{s}_l)^2$ and the string operators

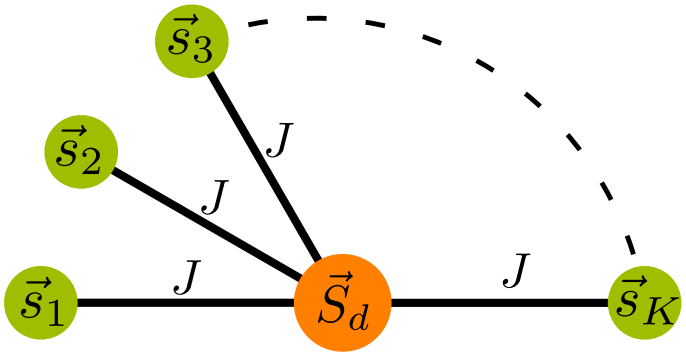

FIG. 2. Zero bandwidth limit of the fixed point Hamiltonian. The central yellow node is the impurity spin, and it is interacting with the local spins of the channels represented as outer green nodes, through a Heisenberg spin-exchange coupling.

$$\pi^{x,y,z} = \sigma_d^{x,y,z} \otimes_{l=1}^{K} \sigma_l^{x,y,z} \ . \tag{9}$$

The π^z acts on the eigenstates $|J^z\rangle$ and reveals the odd-even parity of the eigenvalue J^z, and is hence a parity operator. Interestingly, *the string operator π^z is a Wilson loop operator [26] that wraps around all the nodes of the star graph*:

$$\pi^z = \exp\left[i\frac{\pi}{2} \left(\sigma^z_d + \sum_{l=1}^{K} \sigma^z_l - K \right) \right] = e^{i\pi\left(J^z - \frac{1}{2}K\right)} \tag{10}$$

π^x and π^y mix states of opposite parity. For example, it can be shown that $\pi^x |J^z\rangle = -|J^z\rangle$. These are 't Hooft operators [26].

There are multiple reasons for working with the star graph in particular and zero mode Hamiltonians in general. In the single-channel Kondo model, the star graph is just the two spin Heisenberg, and it reveals the stabilization of the Kondo model ground state, as well as certain thermodynamic properties (e.g., the impurity contribution to the susceptibility) [8, 27–30]. Similarly in the MCK model, the star graph is able to mimic the nature of the RG flows: At weak coupling $J \to 0^+$, the central spin is weakly coupled to the outer spins and prone to screening because of the $s^\pm$ terms in the star graph, and at strong coupling $J \to \infty^-$, the outer spin-half objects tightly bind with the central spin-half object to form a single spin object that interacts with the remaining states through an exchange coupling which is RG relevant, rendering both the terminal fixed points unstable. The true stable fixed point must then lie somewhere in between, and we recover the schematic phase diagram of fig. 1.

The utility of the star graph is due to the fact that *the non-Fermi liquid arises solely from the degeneracy of the ground state manifold of the underlying zero mode Hamiltonian, and the star graph captures this degeneracy in its entirety.* The RG flows of the MCK model have been show to *preserve the degeneracy of the ground state* [23, 31, 32]. The star graph conserves the total spin J^z, and this leads to a ground state degeneracy of $|\frac{K}{2} - S| + 1$ in the $K-$channel spin-S star graph which is preserved under the RG flow. This is qualitatively different from the case of the single-channel Kondo model where the $2-$fold degeneracy of the local moment fixed point crosses over into a stable and unique singlet ground state.

As we will see in a subsequent section, the lowest excitations of the intermediate fixed point is described a non-Fermi liquid phase induced by nearest-neighbour hopping terms between the zeroth sites and the first sites of the conduction channels. The importance of the degeneracy can be shown in the following manner. As mentioned previously, the ground state degeneracy of the more general star graph with a spin-S impurity and K channels is given by $g^S_K = |K - 2S| + 1$. The cases of $K = 2S$, $K < 2S$ and $K > 2S$ correspond to exactly screened, under-screened and over-screened regimes respectively. *The latter two cases correspond to a multiply-degenerate manifold $g^S_K > 1$, and simultaneously have non-Fermi liquid phases [1, 9, 12, 18, 19, 21, 33–43], while the first regime has a unique ground state $g^S_K = 1$ and is described by a local Fermi liquid (LFL) phase [1, 44–47], thereby substantiating the claim that a degeneracy greater than unity leads to non-Fermi liquid physics.* In the following sections, we will show how the inherent quantum-mechanical frustration of singlet order that is present in the Hamiltonian leads to the degenerate ground state manifold and the non-trivial physics of the fixed points in terms of non-Fermi liquid phase, diverging thermodynamic quantities, quantum criticality as well as emergent gauge theories.

III. IMPORTANT PROPERTIES OF THE STAR GRAPH

A. Hamiltonian and wavefunctions

As shown in the previous section, at the heart of multi-channel Kondo there is a star graph problem which is the zero mode of the low energy fixed point Hamiltonian of the Multi channel Kondo. In this section our focus will be on the star graph problem itself. As shown in the Fig.2 above, one central spin ($\vec{S}_d$) is connected with K spins forming a K channel star graph problem corresponding to the K-channel Kondo problem. The Hamiltonian of this above model is given as

$$\begin{aligned} H &= \alpha \vec{S}_d . \sum_{i=1}^{K} \vec{S}_i = \alpha \vec{S}_d . \vec{S} \\ &= \frac{\alpha}{2}(\vec{J}^2 - \vec{S}^2 - \vec{S}_d^2) \ , \quad \alpha > 0. \end{aligned} \tag{11}$$

where $\vec{J} = \vec{S} + \vec{S}_d$ and $\vec{S} = \sum_{i=1}^{K} \vec{S}_i$. One can see that the large psin S can take many possible values as this is made out of K spin 1/2s. We can see $[H, J] = 0 = [H, J^i]$ for $i = x, y, z$, $[J^i, J^j] \neq 0$ for $i \neq j$. Also the operators $\hat{Z} = 2^{K+1} S_d^z \prod_{i=1}^{K} S_i^z$ and $\hat{X} = 2^{K+1} S_d^x \prod_{i=1}^{K} S_i^x$ commutes with the Hamiltonian, $[H, \hat{Z}] = 0 = [H, \hat{X}]$ though $[\hat{Z}, \hat{X}] \neq 0$, in general. Thus we can form the CSCO with H, J, J^z, S, S_d. For a particular value S, J can take two values $S \pm S_d$ with the energies $-\alpha S_d(S_d + 1 \mp J)$ respectively. S_d is fixed thus the energy values only depends on the corresponding J value of the state. As the energy does not depends on the J^z, all $2J + 1$ J^z states labeled by $|S_d, S; J, J^z\rangle$ are degenerate. It is easy to see that the ground state has energy $E = -\alpha S_d(S_d + 1 + J)$ with $J = S - S_d$, thus $E_g = -\alpha S_d(S_{max} + 1)$ with S taking the maximum possible value $S_{max} = K/2$.

1. Ground state wavefunction

Above calculations show star graph with K channels has K-fold ground state degeneracy, states labeled as $|S_d, S; J, J^z\rangle$ where J^z takes $K = 2J + 1$ distinct values, $J^z = \{-J, \cdots, +J\}$. Here our goal is to find the wavefunction in the fundamental spin basis $|S_d^z, S_1^z, \cdots, S_K^z\rangle$. To achieve that we use the Clebsch-gordon coefficients, we know for two spins j_1 and j_2 with total spin J and $J^z = M$ one can expand the state as

$$|j_1, j_2; J, M\rangle = \sum_{\substack{m_1 = \{-j_1, \cdots, j_1\} \\ m_2 = \{-j_2, \cdots, j_2\}}} \mathcal{C}^{j_1, m_1; j_2, m_2}_{j_1, j_2; J, M} |j_1, m_1; j_2, m_2\rangle \tag{12}$$

where $j_1^z = m_1$ and $j_2^z = m_2$ and $\mathcal{C}^{j_1, m_1; j_2, m_2}_{j_1, j_2; J, M}$ is the Clebs-Gordon coefficient. In our problem two spins S_d and S are forming one large spin J represented by the state $|S_d, S; J, J^z\rangle$, in the ground state $J = S - 1/2$. Thus the ground state $|S_d, S; (S - \frac{1}{2}), M\rangle \equiv |\alpha\rangle$ can be expanded as

$$|\alpha\rangle = \sum_{\substack{m_1 = \{-S_d, \cdots, S_d\} \\ m_2 = \{-S, \cdots, S\}}} \mathcal{C}^{S_d, m_1; S, m_2}_{S_d, S; J, M} \ |S_d, m_1\rangle \otimes |S, m_2\rangle, \tag{13}$$

Because in the ground state S is maximum, the state $|S, S^z\rangle$ can be decomposed in terms of a two spin problem of spin 1/2 and $S - 1/2$ forming the state $|1/2, S - 1/2; S, S^z\rangle$ which can be further expanded in the basis $|1/2, m_1'\rangle \otimes |S - 1/2, m_2'\rangle$ where m_1', m_2' are the z-components of the spin 1/2 and $S - 1/2$. Next we decompose the state $|S - 1/2, m_2'\rangle$ in further smaller spin problem and so on. This way we finally arrive at the ground state wavefunction in terms of the fundamental basis $|S_d^z, S_1^z, \cdots, S_K^z\rangle$, give as

$$|S_d, S; J, M\rangle = \sum_{S_d^z, \{S_i^z\}} \mathcal{D}_{S_d^z, \{S_i^z\}} |S_d^z, S_1^z, \cdots, S_K^z\rangle \tag{14}$$

where $\{S_i^z\} \equiv (S_1^z, \cdots, S_K^z)$ and the coefficient $\mathcal{D}_{S_d^z, \{S_i^z\}}$ is given as

$$\mathcal{D}_{S_d^z, \{S_i^z\}} = \sum_{\substack{m_2 = [-S, S] \\ m_4 = [-(S-1/2), (S-1/2)] \\ \vdots \\ m_{2N-4} = [-1, 1]}} \mathcal{M}^{S_d^z, S_1^z, \ \cdots, S_K^z}_{m_2, m_4, \ \cdots, m_{2N-2}} \ , \tag{15}$$

and further the coefficients $\mathcal{M}^{S_d^z, S_1^z, \ \cdots, S_K^z}_{m_2, m_4, \ \cdots, m_{2N-2}} \equiv \Sigma$, are made out of the products of Clebsh-Gordon Coefficients

$$\Sigma = \mathcal{C}^{S_d, S_d^z; S, m_2}_{S_d, S; J, M} \ \mathcal{C}^{S_1, S_1^z; (S-1/2), m_4}_{S_1, (S-1/2); S, m_2} \cdots \mathcal{C}^{S_{K-1}, S_{K-1}^z; S_K, S_K^z}_{S_{K-1}, S_K; 1, m_{2N-4}} \tag{16}$$

Using these wavefunctions we can calculate various entanglement features of this star graph problem.

B. Entanglement properties

Using the above exact wavefunctions we can numerically compute various entanglement properties of this star graph model.

1. Impurity entanglement entropy

Here we are interested in finding the entanglement of the central impurity spin with the rest of the multi-channel bath zero mode. We know that for multi-channel case the ground state is degenerate, thus for each degenerate state we can calculate the entanglement entropy. As we have already discussed for N_{ch} number of channels there are N_{ch} number of degenerate ground states, labeled by the J_z quantum number.

For single channel case the the ground state is unique and is

$$|J = 0, J_z = 0\rangle = \frac{1}{\sqrt{2}}(|\uparrow_d \downarrow_0\rangle - |\downarrow_d \uparrow_0\rangle) \tag{17}$$

Thus, one can easily calculate the reduced density matrix of the impurity by tracing out the 0^{th} state. From that reduced denisty matrix the entanglement entropy is $\log 2$, which is maximum possible for a spin-1/2.

Next, we are interested in findig this entanglement entropy for the multi-channel case $N_{ch} > 1$. We have generated the degenerate ground states analytically using the Clebsch-Gordon coefficients. On this wavefunctions we do various entanglement and correlation studies. We start with the ground state wavefunction, $|\psi_g\rangle_{J_z} = |1/2_d, S; J, J_z\rangle$, starting with one of those degenerate ground states labeled by J_z we calculate the density matrix.

$$\rho_{J_z} = |\psi_g\rangle_{J_z}\langle\psi_g|_{J_z} \tag{18}$$

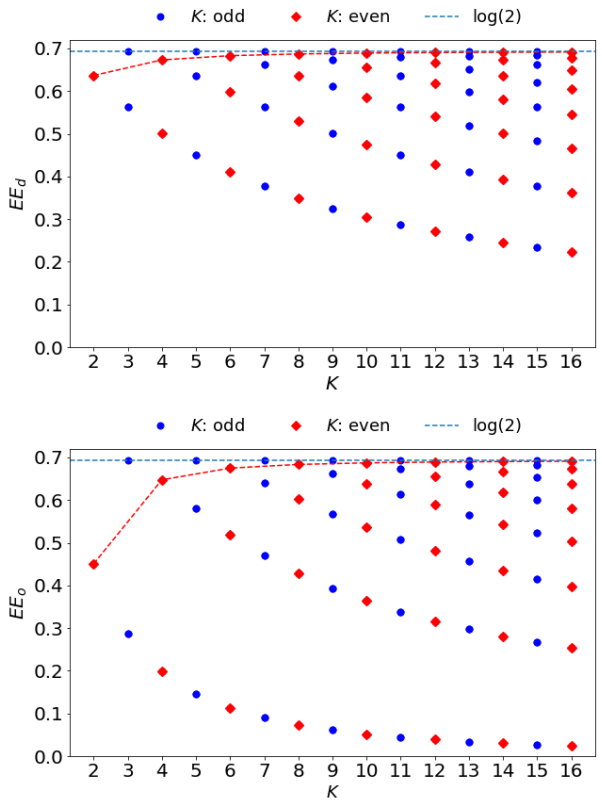

FIG. 3. Y-axis shows the impurity entanglement entropy with the rest and X-axis shows the number of channels N_{ch}. For one value of $N_{ch} > 1$, there are N_{ch} degenerate ground states and their corresponding impurity entanglement entropy.

Using the wavefunction we can do the partial tracing on the impurity spin to get the reduced denisty matrix of the rest. From that we get entanglement entropy for different number of channels. For even number of channel cases J_z and $-J_z$ sector has same entanglement entropy. For the case of odd N_{ch} there also $\pm J_z$ sectors shares same entanglement entropy, but there is a state $J_z = 0$ which has entanglement entropy $\log 2$. Thus from the above we can see that $J_z = 0$ state corresponding to odd number of channels shows perfect screenig interms of the maximum entanglement entropy and $J_z = 0$ magnetization.

2. *Mutual Information*

Mutual information between two sub-systems A, B is defined as,

$$I^2(A:B) = S_A + S_B - S_{A\cup B} \tag{19}$$

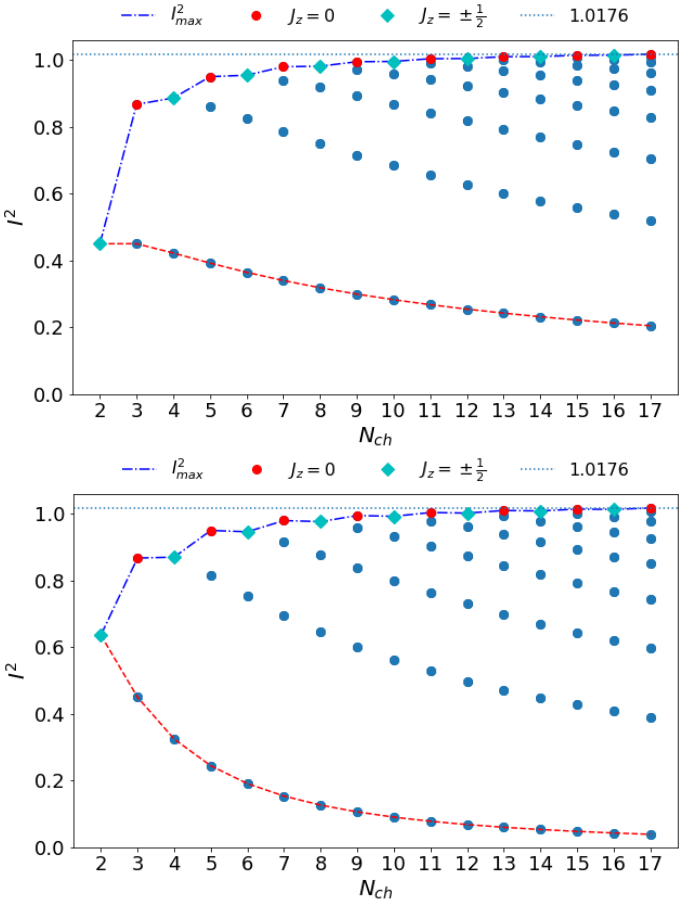

FIG. 4. *Left:* Y-axis is the mutual information between the impurity-spin and one outer spin and x-axis is the number of channel N_{ch}. *Right:* This shows the variation of mutual information between two outer spins.

We first study the mutual information between the impurity-spin and one outer spin $I^2(d:o)$. Because all the outer spins are symmetric, the mutual information between impurity-spin with any one outer spin is same. Next we calculate the mutual information between two outer spin $I^2(o:o)$. One can see that the maximum mutual information for both the cases are from the $(J_z)_{min}$ state. For odd number of channels $(J_z)_{min} = 0$ and for even number of channels $\pm(J_z)_{min} = \pm 1/2$. And the minimum mutual information corresponds to the $\pm(J_z)_{max} = \pm J$ state.

As can be seen from the above Figure.4 that both the maximum mutual information of $I^2(d:o)$ and $I^2(o:o)$ try to saturate near the same value. Thus in the lowest J_z sector the entanglement distribution between impurity and outer vs outer and outer is same. Which suggests that even though there were no coupling among the outer spins explicitly, there are entanglement among them. The minimum of the mutual information coming from the largest J_z sector, the $I^2(o:o)$ corresponding to this sector asymptotically approach zero for large N_{ch} limit. Which shows that in the large channel limit $N_{ch} \gg 1$ though the $min\ I^2(o:o)$ pparoach zero the $min\ I^2(d:o)$

3. *Tripartite information*

Apart from Mutual information we can calculate the tripartite information also. This tripartite information is defined among three sub-systems A, B, C , as

$$I^3_{A,B,C} = (S_A + S_B + S_C) - (S_{AB} + S_{BC} + S_{CA}) + S_{ABC} \tag{20}$$

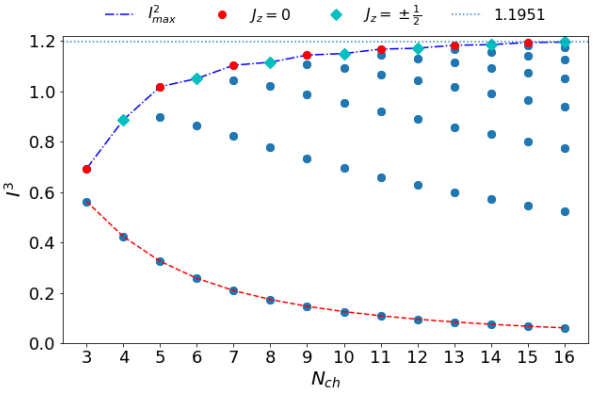

FIG. 5. This plot shows the variation of the tripartite information with the number of channels N_{ch}.

Our tripartite information measure (Fig.5) among the outer spins shows that the just like the mutual information the minimum tripartite information asymptotically approaches zero in the $N_{ch} \gg 1$ limit. Same is the case for 4-partite information also.

4. *I_N vs N*

Here we are intersted in understading the entanglement dristribution among different number of outter spins. To find that out we take a multi-channel star graph model with N_{ch} noumber of outer spins. We calculate different multi partite inforamtions $I^m, m \in \{2, \cdots, N_{ch}\}$ on it's N_{ch} degenerate ground states.

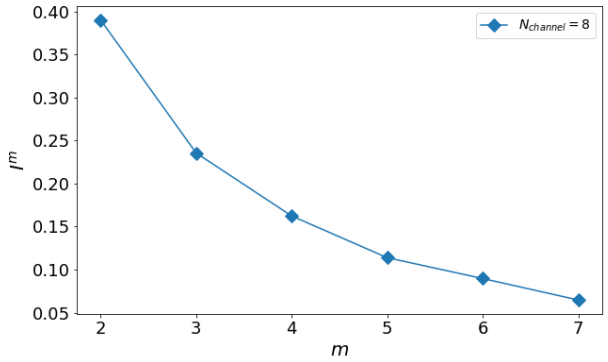

FIG. 6. This figure shows how the $m-partite$ information varies with m showing the entanglement distribution amond different number of outer-spins.

Our above study (Fig.6) shows that the mutual imformation has the maximum value and higher odere multiparite informations is smaller and smaller approaching zero.

C. Correlation Studies

1. *Quantum energy*

Here we are interested in the energy expectation value arising from the quantum fluctuation part of the Hamiltonian (**??**). We define Ising energy E_{ising} and quantum energy E_Q in the ground state $|\psi_g\rangle$ as,

$$E_{ising} = |\langle\psi_g|\mathcal{H}_0^c|\psi_g\rangle| \tag{21}$$

$$E_Q = |\langle\psi_g|\mathcal{H}_0^Q|\psi_g\rangle| = |E_g| - |E_{ising}| = \frac{\alpha(S+1)}{2} - |E_{ising}| \ . \tag{22}$$

This quantum energy E_Q is generated by the spin-flips between the impurity spin and the outer spin. Thus it is interesting to findout how this quantum energy changes with the increase of the number of channels (N_{ch}). Another important parameter is the Quantum enrgy per channel, $e_Q = |E_Q|/N_{ch}$, and it's variation towards the infinity channel limit. We know in the gorund state $N_{ch} = 2S$ thus,

$$\begin{aligned} e_Q &= \frac{\alpha(S+1)}{4S} - \frac{|E_{ising}|}{2S} \ , \\ &= \frac{\alpha}{4} - \frac{1}{N_{ch}}\left(|E_{ising}| - \frac{\alpha}{2}\right) \ , \end{aligned} \tag{23}$$

Thus from the above equation of quantum energy per channel one can see that in the inifinity-channel limit $N_{ch} \to \infty$,

$$e_Q = \frac{\alpha}{4} - \frac{|E_{ising}|}{N_{ch}} < \frac{\alpha}{4} \ , \tag{24}$$

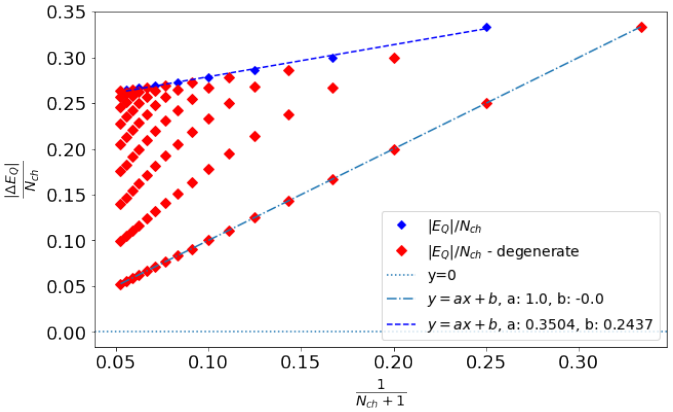

FIG. 7. This shows the variation of quantum energy per channel with $1/N$, where $N = N_{ch}+1$ is the total number of spins in the systems including the impurity spins.

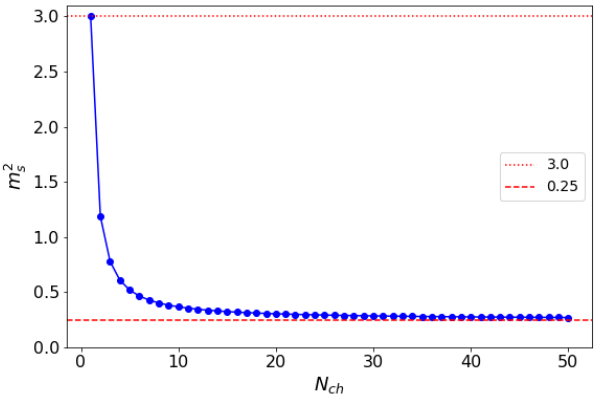

FIG. 8. This shows how the staggered magnetization changes with the number of channels N_{ch}.

2. *Correlation study*

Here we want to calculate various correlation functions in the ground state. We start with the expectation value of J_z^2 in the ground state $|\psi_g\rangle$,

$$j_z^2 = \frac{1}{N_{ch}}\langle\psi_g|J_z^2|\psi_g\rangle = \frac{1}{N_{ch}}\left[J^2 - (J_x^2 + J_y^2)\right] ,$$
$$= \frac{1}{N_{ch}}\left[\frac{(N_{ch}^2-1)}{4} - (J_x^2 + J_y^2)\right] \quad (25)$$

$$\langle\psi_g|J_z^2|\psi_g\rangle_{max} = \left(\frac{N_{ch}-1}{2}\right)^2 ,$$
$$\langle\psi_g|J_z^2|\psi_g\rangle_{min} = \left(\frac{N_{ch}-(N_{ch}-1)}{2}\right)^2 = \frac{1}{4} , \text{ for } N_{ch} \text{ even.}$$
$$= 0 , \text{ for } N_{ch} \text{ odd} \quad (26)$$

Thus,

$$\langle (J_x)^2 + (J_y)^2\rangle_{max} = \langle J^2\rangle - \langle J_z^2\rangle_{min} ,$$
$$= \frac{N_{ch}^2-1}{4} - \frac{1}{4} = \frac{N_{ch}^2-2}{4} , \text{for } N_{ch} \text{ even}$$
$$= \frac{N_{ch}^2-1}{4} , \text{for } N_{ch} \text{ odd}$$

Which shows, for single channel case $N_{ch} = 1$, this quntum fluctuation expectation value vanishes, while for multi-channel this takes non-zero values. Thus

$$\frac{1}{N_{ch}}\langle (J_x)^2 + (J_y)^2\rangle_{max} = \frac{N_{ch}}{4} - \frac{1}{2N_{ch}} , \text{for } N_{ch} \text{ even}$$
$$= \frac{N_{ch}}{4} - \frac{1}{4N_{ch}} , \text{for } N_{ch} \text{ odd}$$

Thus in the large channel number limit $N_{ch} \gg 1$, one can see that

$$\frac{1}{N_{ch}}\langle (J_x)^2 + (J_y)^2\rangle_{max} \to \frac{N_{ch}}{4} , \text{ for both even and odd } N_{ch} \quad (27)$$

J_z can take values $\{-J, -J+1, \cdots, J-1, J\}$ in the ground state, where $J = S - 1/2 = (N_{ch}-1)/2$.

3. *Staggerred magnetization*

One can analytically check the single channel Kondo results. $N_{ch} = 1$, thus here the ground state is unique.

$$|\psi_g\rangle = \frac{1}{\sqrt{2}}\Big(|\uparrow\downarrow\rangle - |\downarrow\uparrow\rangle\Big) = |J=0, J_z=0\rangle \quad (28)$$

Thus in this ground state $\langle J_z\rangle = 0$ and the entanglement entropy is $\log 2$ the maximum value. Now we define a staggered magnetization (8) operator M_s measure,

1. For the single channel case both the $\vec{S}_d$ and $\vec{S}$ are spin-1/2 object and the total spin is defined as $\vec{J} = \vec{S}_d + \vec{S}$. Here $\vec{S}$ is the total outer spin.

$$M_s^2 = \langle\psi_g|(\vec{S}_d - \vec{S})^2|\psi_g\rangle = \langle\psi_g|2(\vec{S}_d^2 + \vec{S}^2) - \vec{J}^2|\psi_g\rangle$$
$$= 2\langle\psi_g|\vec{S}_d^2 + \vec{S}^2|\psi_g\rangle$$
$$= 3 \quad (29)$$

2.

$$M_s^2 = \langle\psi_g|(\vec{S}_d - \vec{S})^2|\psi_g\rangle = \langle\psi_g|2(\vec{S}_d^2 + \vec{S}^2) - \vec{J}^2|\psi_g\rangle$$
$$= \left\langle\psi_g\middle|2\left(\frac{3}{4} + \frac{N_{ch}(N_{ch}+2)}{4}\right) - \frac{(N_{ch}+1)(N_{ch}-1)}{4}\middle|\psi_g\right\rangle$$
$$= \frac{N_{ch}^2}{4} + N_{ch} + \frac{7}{4} \quad (30)$$

Thus, staggered magnetization squared per channel,

$$m_s^2 = \frac{M_s^2}{N_{ch}^2} = \frac{1}{4} + \frac{1}{N_{ch}} + \frac{7}{4N_{ch}^2} \xrightarrow{N_{ch}\gg 1} \frac{1}{4} + \frac{1}{N_{ch}} \quad (31)$$

$$\frac{\vec{J}^2}{N_{ch}^2} = \frac{(\vec{S}_d + \vec{S})^2}{N_{ch}^2} = \frac{N_{ch}^2-1}{4N_{ch}^2} \xrightarrow{N_{ch}\gg 1} \frac{1}{4} .$$

Using the $SU(2)$ property of our problem, we can define m_s for each spatial direction, in 3D there are three independent spatial direction.

$$\langle (m_s^x)^2 \rangle = \langle (m_s^y)^2 \rangle = \langle (m_s^z)^2 \rangle = \frac{1}{3} m_s^2 \ , \tag{32}$$

We define $m_Q^2 = m_s^2 - 1/4$ which in the the large N_{ch} limit becomes $1/N_{ch}$ and eventually vanishes in the $N_{ch} \to \infty$ limit.
Thus to summarize,

1. In the single channel problem, $\langle (m_s^z)^2 \rangle = 1$.
2. In the multi-channel case, $\langle (m_s^z)^2 \rangle = \frac{1}{3N_{ch}} + \frac{1}{12} + \frac{7}{12N_{ch}^2} \xrightarrow{N_{ch} \gg 1} \frac{1}{12} + \frac{1}{3N_{ch}} \to \frac{1}{12}$. This show partial screening.

Thus it is important to find the scaling of

1. M_s^2 vs N_{ch}.
2. Uncompensated Quantum Fluctuation vs N_{ch}.

D. Thermal entropy

We take the star graph Hamiltonian and do the exact diagonalization and find the entire eigenspectrum. Using the full eigenspectrum we calculate the partition function $Z = \sum_i e^{-\beta E_i}$, where E_i is the energy of the i^{th} state. One can rewrite this partition function in terms of the state degeneracies as $Z = \sum_\epsilon d(\epsilon) e^{-\beta\epsilon}$, where $d(\epsilon)$ is the degeneracy of the state with energy ϵ. Thus the free energy is given as $\mathcal{F} = -k_B T \log Z$.
Thermal entropy is defined as $S = -(\frac{\partial \mathcal{F}}{\partial T})_H$, where H represents a constant magnetic field. In ourcase we will be interested in the zero field case.

$$\begin{aligned} \mathcal{F} &= -k_B T \log Z \\ S &= -(\frac{\partial \mathcal{F}}{\partial T}) = -k_B \log Z - k_B T \frac{1}{Z} \frac{dZ}{dT} \end{aligned} \tag{33}$$

Now

$$\begin{aligned} Z &= \sum_\epsilon d(\epsilon) e^{-\beta\epsilon} \\ \implies \frac{dZ}{dT} &= \sum_\epsilon d(\epsilon) e^{-\beta\epsilon} (-\epsilon) \frac{d\beta}{dT} = \sum_\epsilon d(\epsilon) e^{-\beta\epsilon} \frac{\epsilon}{k_B T^2} \\ &= k_B \sum_\epsilon \epsilon d(\epsilon) e^{-\beta\epsilon} \beta^2 \end{aligned} \tag{34}$$

Thus we get

$$S = -k_B \log \sum_\epsilon d(\epsilon) e^{-\beta\epsilon} - \frac{1}{\beta} \frac{k_B \sum_\epsilon \epsilon d(\epsilon) e^{-\beta\epsilon} \beta^2}{\sum_\epsilon d(\epsilon) e^{-\beta\epsilon}}$$

$$\lim_{\beta \to \infty} S = -k_B \log_2 d(\epsilon_G) \ \text{, and} \ \lim_{\beta \to 0} S = -k_B \log \sum_\epsilon 1 \tag{35}$$

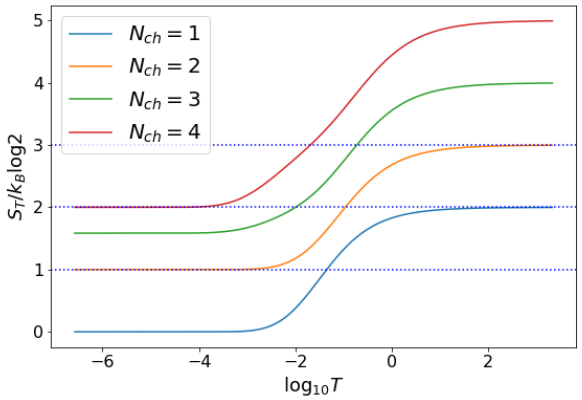

FIG. 9. This shows the variation of thermal entropy with the temperature.

Thus at the extreme temperature it is easy to calculate the thermal entropy, but it is difficult to visualize for any intermediate temperatures. Thus we plot the thermal entropy (unit $\log 2$) for different temperatures and for different channels in Fig.9. This shows at the extreme temperature the thermal entropy saturates and at the intermediate temperature it changes from one to the other like a soliton like solution. At low temperature the thermal entropy in the unit of $\log 2$ is not always quantized but at high temperature it is. To understand this let's say at low temperature $S_T/k_B \log T = \Omega = \log_2 d(\epsilon_G)$. Here $d(\epsilon_G)$ is always integer and equal to the channel number K. Thus

$$d(\epsilon_G) = 2^\Omega = K \tag{36}$$

From our study we can see that for some channel number we get $S_T/k_B \log T$ to be integer. One can easily see that those $K = 2^n$ channel cases, n is an integer will have integer thermal entropy. Thus between m and $m+1$ integer thermal entropy plateau there will be $(2^m - 1)$ number of fractional thermal entropy plateau, which is always odd.

E. Degree of compensation: a measure of the frustration

One can quantify the amount of screening of the local moment at the impurity site by defining a degree of compensation κ. Such a quantity also measures the inherent singlet frustration in the problem: the higher the degree of compensation, the better the spin can be screened into a singlet and lower is the frustration. It is given by the antiferromagnetic correlation existing between the impurity spin and conduction electron channels:

$$\Gamma \equiv -\left\langle \vec{S}_d \cdot \vec{s}_{\rm tot} \right\rangle \tag{37}$$

where $\vec{s}_{\rm tot} = \sum_l \vec{s}_l$. The expectation value is calculated in the ground state. Since the inner product is simply the ground state energy of a spin-S impurity $K-$channel MCK model in units of the exchange coupling J, we have

$$\Gamma = \frac{1}{2}\left[l^2_{\rm imp} + l^2_c - g^S_K\left(g^S_K - 1\right)\right] \tag{38}$$

$l^2_{\rm imp} = S(S{+}1)$ is the length-squared of the impurity spin. Similarly, $l^2_c = \frac{K}{2}\left(\frac{K}{2}+1\right)$ is the length-squared of the total conduction bath spin. $g^S_K = |\frac{K}{2} - S|{+}1$ is the ground state degeneracy. We will explore the three regimes of screening by defining $K = K_0 + \delta, S = \frac{K_0}{2} - \delta$. $\delta = 0$ represents the exactly-screened case of $K = 2S = K_0$. Non-zero δ represents either over- or under-screening. In terms of K_0 and δ, the degree of compensation becomes

$$\Gamma = \frac{1}{4}\left[(K_0+1)^2 - (|\delta|+1)^2\right] \tag{39}$$

For a given K_0, the degree of compensation is maximised for exact screening $\delta = 0$, and is reduced for $\delta \neq 0$. This shows the inability of the system to form a unique singlet ground state and reveals the quantum-mechanical frustration inherent in the zero mode Hamiltonian and therefore in the entire problem. The degree of compensation is symmetric under the Hamiltonian transformation $\delta \to -\delta$, and this represents a duality transformation between over-screened and under-screened MCK models. This topic will be discussed in more detail later.

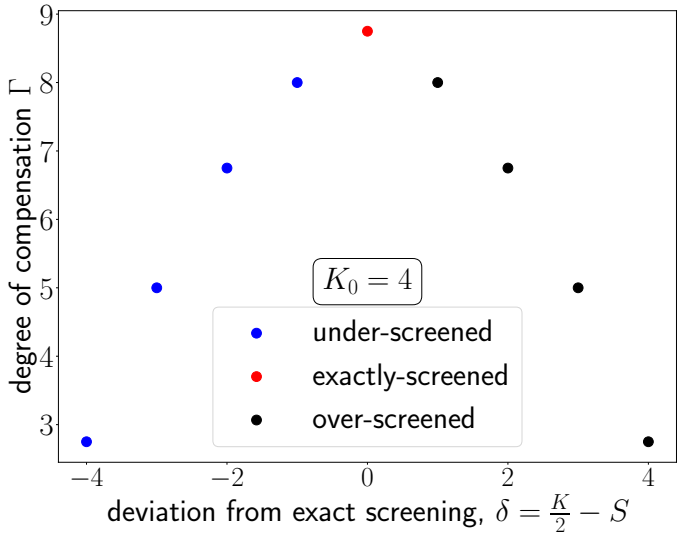

FIG. 10. Variation of the degree of compensation as we tune the system from under-screening to over-screening. The maximum spin compensation occurs at exact-screening $\delta = 0$.

F. Impurity magnetization and susceptibility: Quantum criticality of overscreened MCK model

The channel isotropic MCK model is critical; any perturbation away from the perfectly symmetric model in terms of anisotropy is relevant, as shown in section VIII A [23, 48, 49]. This critical nature leads to several signatures that can be obtained directly from the star graph. These signatures include a discontinuity in the impurity magnetization at zero temperature in the limit of the external field going to zero, and a diverging susceptibility as temperature goes to zero.

We insert a magnetic field that acts only on the impurity and then diagonalize the Hamiltonian.

$$H(h) = J^* \vec{S}_d \cdot \vec{s}_{\rm tot} + h S^z_d \tag{40}$$

The Hamiltonian commutes with $s_{\rm tot}$, so it is already block-diagonal in terms of the eigenvalues M of $s_{\rm tot}$. M takes values in the range $[M_{\rm min}, M_{\rm max}]$, where $M_{\rm max} = K/2$ for a $K-$channel Kondo model, and $M_{\rm min} = 0$ if K is even, otherwise $\frac{1}{2}$. Within each block, the Hamiltonian splits into independent 2×2 blocks characterized by eigenvalues of the total spin operator $J^z = S^z_d + s^z_{\rm tot}$. Defining $\alpha = \frac{1}{2}(Jm + h) + \frac{J}{4}$ and $x^M_m = M(M+1) - m(m+1)$, the partition function can be written as

$$Z(h) = \sum_{M=M_{\rm min}}^{M_{\rm max}} r^K_M \left[\sum_{\substack{m=-M,\\ m\in\mathbb{Z}}}^{M-1} 2e^{\beta\frac{J}{4}} \cosh\beta\sqrt{J^2 x^M_m/4 + \alpha^2} + 2e^{-\beta JM/2}\cosh\beta h/2\right] \tag{41}$$

Here, $\beta = \frac{1}{k_B T}$, M sums over the eigenvalues of $s_{\rm tot}$ while m sums over $J^z - \frac{1}{2}$ and the additional degeneracy factor r^K_M arises from the possibility that there are multiple subspaces defined by $s_{\rm tot} = M$. This multiplicity is given by

$$r^K_M = {}^{K-1}C_{K/2-M} \tag{42}$$

To calculate the impurity magnetic susceptibility, we will use the expression

$$\chi = \frac{1}{\beta}\lim_{h\to 0}\left[\frac{Z(h)''}{Z(h)} - \left(\frac{Z(h)'}{Z(h)}\right)^2\right] \tag{43}$$

where the $'$ indicates derivative with respect to h. For brevity, we define $\theta_M = \beta J(M+\frac{1}{2})/2$ and $\Sigma_M = \sum^{M-1}_{\substack{m=-M,\\ m\in\mathbb{Z}}}(m+\frac{1}{2})^2$. At low temperature $\beta\to\infty$, only the highest value $M_{\rm max}$ will survive:

$$Z \to 2r^K_{M_{\rm max}} M_{\rm max} e^{\beta\frac{J}{2}(M_{\rm max}+1)} \tag{44}$$

$$Z'' \to r^K_{M_{\rm max}}\left(\frac{\beta}{2(M_{\rm max}+\frac{1}{2})}\right)^2 e^{\beta\frac{J}{2}(M_{\rm max}+1)}\Sigma_{M_{\rm max}} \tag{45}$$

$$\chi \to \frac{\beta\Sigma_{\rm max}}{2M_{\rm max}(2M_{\rm max}+1)^2} = \frac{\beta(K-1)}{12(K+1)} \sim \frac{1}{T} \tag{46}$$

This non-analyticity in a response function is a signature of the critical nature of the Hamiltonian. This is

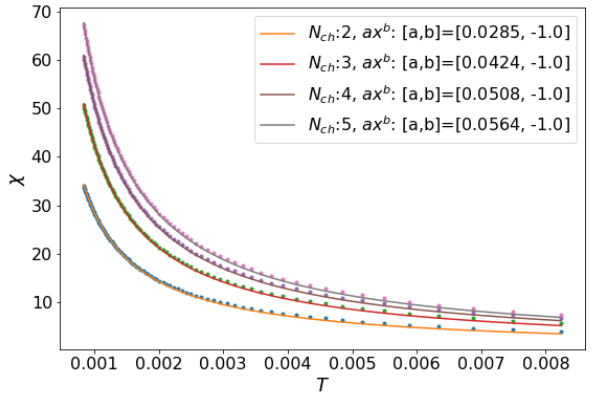

FIG. 11. Impurity susceptibility vs temperature.

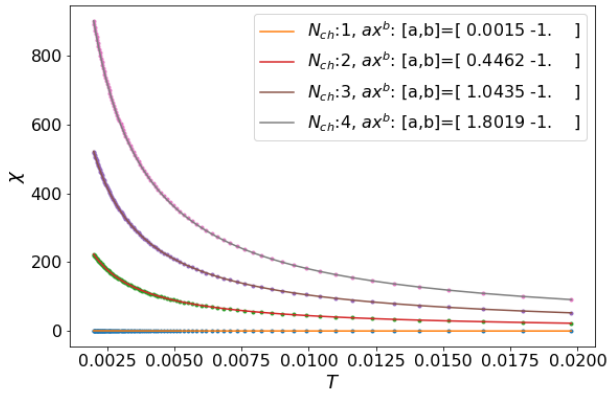

FIG. 12. Outer susceptibility vs temperature.

in contrast to the behaviour in the non-critical exactly-screened fixed point where the ground state is unique. There, the susceptibility becomes constant at low temperatures: $\chi(T \to 0) = \frac{W}{4T_K}$, T_K being the single-channel Kondo temperature and W the Wilson number [8, 29, 45, 50]. We have checked the case of general spin-S impurity numerically (see fig. 11), and all exactly-screened models show a constant impurity susceptibility at $T \to 0$, while the over-screened and under-screened cases show a diverging impurity susceptibility in the same limit.

For completeness, we have also studied (numerically) the susceptibility coming from a magnetic field on the outer spins. The results are shown in fig. 12, and we see a similar universality; all cases of inexact screening have a susceptibility that diverges as T^{-1}, while the case of exact screening shows a constant screening at low temperatures.

Another non-analyticity arises when we consider the impurity free energy and the magnetization. The thermal free energy is given by

$$F(h) = -\frac{1}{\beta} \ln Z(h) = -\frac{1}{\beta} \ln \sum_{E_n} e^{-\beta E_n} \tag{47}$$

At $T \to 0$, only the most negative energy $E_{\min}$ survives. Assuming a non-degenerate ground state for $h \neq 0$, the zero temperature free energy becomes

$$F(h \neq 0, T \to 0) = -\frac{1}{\beta} \ln e^{-\beta E_{\min}} = E_{\min} \tag{48}$$

In the star graph Hamiltonian with $K-$channels and in the presence of a field on the impurity (eq. 40), the ground state energy will be one of the negative eigenvalues:

$$\lambda^{M,h}_{m,-} = -\frac{J}{4} - \frac{1}{2}\sqrt{J^2(M+1/2)^2 + h^2 + 2hJ(m+1/2)} \tag{49}$$

The minimum eigenvalue is obtained by maximizing $h(m+1/2)$. For $h > 0$, the ground state is renormalised for the most positive value of m, which is $M-1$. On the other hand, for $h < 0$, it occurs for $m = -M$, because that is the most negative value it can take. Among all the values of M, the global ground state is at the largest value of M, $K/2$. Therefore, the minimal energy eigenvalue is

$$E_{\min} = -\frac{J}{4} - \frac{1}{2}\sqrt{J^2(K+1)^2/4 + h^2 + |h|J(K-1)} \tag{50}$$

The first derivative of the free energy with respect to the field gives

$$F'(h \neq 0, T \to 0) = -\frac{2h + J(K-1)\text{sign}(h)}{4\sqrt{\frac{J^2}{4}(K+1)^2 + h^2 + |h|J(K-1)}} \tag{51}$$

There we used the result that the derivative of $|x|$ is $\text{sign}(x)$. If we now take h to zero from both directions, we get the magnetization of the impurity

$$m = F'(h \to 0^{\pm}, T \to 0) = \mp\frac{1}{2}\frac{(K-1)}{(K+1)} \tag{52}$$

The magnetization is therefore discontinuous as $h \to 0$; it goes to different values depending on the direction in which we take the limit. The non-analyticity for $K > 1$ occurs because there is at least one pair of ground state with non-zero parity π^z and magnetic field is able to flip one ground state into the state of opposite parity. This available space for scattering is simply the frustration that we discussed earlier. This argument, along with the diverging susceptibility for the over- and under-screened cases, makes it clear that *the non-analyticity and hence the critical nature of the fixed point arise because of the ground state degeneracy, and is therefore a feature of all over-screened and under-screened models.* Indeed, we have checked numerically (see fig. 13) that the non-analyticity exists for $\delta \neq 0$, where $\delta = \frac{K}{2} - S$ is the deviation from exact screening. For $\delta = 0$, the ground state is unique and un-frustrated, so the external magnetic field has no parity-inverted pair to flip across.

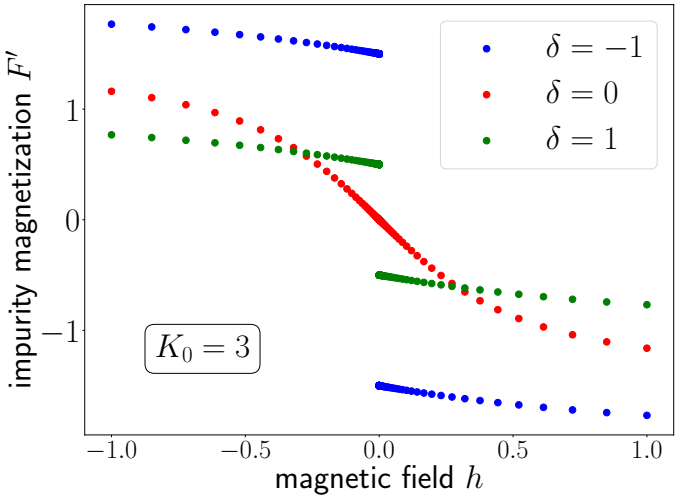

FIG. 13. Behaviour of the impurity magnetization for three values of $(K, 2S) = (2,4), (3,3), (4,2)$. Only the case of $K = 2S = 3\,(\delta = 0)$ is analytic near zero. The non-analyticity of the other cases arises because of the frustration brought about by the degeneracy of the star graph ground state.

G. Impurity magnetization in terms of parity operators

Just like the complete string operator π^z, the modified string operator $\sigma_d^z \pi^z$ is also a Wilson loop operator that wraps around only the outer nodes of the star graph:

$$\pi_c^z \equiv \sigma_d^z \pi^z = \exp\left[i\frac{\pi}{2}\left(\sum_{l=1}^{K}\sigma_l^z - K\right)\right] \tag{53}$$

The expectation value of the impurity magnetization along a particular direction and in specific ground states can be related to the 't Hooft operator defined under eq. 10. We will work in the state comprised of two adjacent eigenstates of J^z:

$$|g_{J^z}^{\theta}\rangle \equiv \frac{1}{\sqrt{2}}\left(|J^z\rangle + e^{i\theta}\,|J^z+1\rangle\right), \quad J^z < \frac{1}{2}(K-1) \tag{54}$$

The expectation value of the impurity magnetization operator σ_d^x can be expressed as

$$\langle\sigma_d^x\rangle \equiv \langle g_{J^z}^{\theta}|\sigma_d^x|g_{J^z}^{\theta}\rangle = -\langle J^z+1|\pi_c^x|-J^z\rangle + \text{h.c.} \tag{55}$$

This expression relates the observable impurity magnetization to the topological 't Hooft operator [51]. Evaluating the matrix elements gives

$$\langle\sigma_d^x\rangle = -\frac{\sqrt{K^2-(2J^z+1)^2}}{2(1+K)}\cos\theta \tag{56}$$

Performing a similar calculation reveals that the impurity magnetizations along y and z in the same state are given by

$$\langle\sigma_d^y\rangle = -\frac{\sqrt{K^2-(2J^z+1)^2}}{2(1+K)}\sin\theta, \quad \langle\sigma_d^z\rangle = -\frac{2J^z+1}{(1+K)} \tag{57}$$

Combining eqs. 56 and 57, we find

$$\cos^2\theta\,(\langle\sigma_d^x\rangle)^2 + \sin^2\theta\,(\langle\sigma_d^y\rangle)^2 + \frac{1}{4}(\langle\sigma_d^z\rangle)^2 = \frac{1}{4}\left(\frac{K}{1+K}\right)^2 \tag{58}$$

This relation constrains the values of the magnetization along all the directions: the x and y magnetization values have already been shown to be related to the 't Hooft operators π^x and π^y and the magnetization along z is therefore constrained in terms of the 't Hooft operators and the quantized function on the right-hand side (the function is quantized because K can only take integer values).

IV. EFFECT OF CONDUCTION BATH EXCITATIONS ON THE FIXED POINT THEORY

A. Non-Fermi liquid signatures in momentum space

Obtaining the effective Hamiltonian involves obtaining the low energy excitations on top of the ground state of the star graph. The large-energy excitations are ones that involve spin flips. This guides the separation of the Hamiltonian into a diagonal and an off-diagonal piece:

$$H = H_d + V = \underbrace{H_0 + JS_d^z s_{\text{tot}}^z}_{H_d} + \underbrace{\frac{J}{2}S_d^+ s_{\text{tot}}^- + \text{h.c.}}_{V+V^\dagger} \tag{59}$$

We define V as the interaction term that decreases s_{tot}^z by 1: $V\,|s_{\text{tot}}^z\rangle \to |s_{\text{tot}}^z - 1\rangle$. Similarly, we define $V^\dagger\,|s_{\text{tot}}^z\rangle \to |s_{\text{tot}}^z + 1\rangle$. The effective Hamiltonian that has the states $|S_d^z, s_{\text{tot}}, s_{\text{tot}}^z\rangle$ as eigenstates are

$$H_{\text{eff}} = H_d + V\frac{1}{E_{\text{gs}} - H_d}V = H_d + \frac{J}{2}S_d^+ s_{\text{tot}}^- \frac{1}{E_{\text{gs}} - JS_d^z s_{\text{tot}}^z - H_0}\frac{J}{2}S_d^- s_{\text{tot}}^+ + \frac{J}{2}S_d^- s_{\text{tot}}^+ \frac{1}{E_{\text{gs}} - JS_d^z s_{\text{tot}}^z - H_0}\frac{J}{2}S_d^+ s_{\text{tot}}^- \tag{60}$$

This is obtained from the Schrodinger equation for the ground state. If we expand the ground state in terms of $|S_d^z, s_{\rm tot}, s_{\rm tot}^z\rangle$, we have $|\Psi_{\rm gs}\rangle = \sum_{S_d^z, s_{\rm tot}, s_{\rm tot}^z} C_{S_d^z, s_{\rm tot}, s_{\rm tot}^z} |S_d^z, s_{\rm tot}, s_{\rm tot}^z\rangle$. The Schrodinger equation for the ground state can be written as

$$E_{\rm gs}|\Psi_{\rm gs}\rangle = H|\Psi_{\rm gs}\rangle = (H_d + V)|\Psi_{\rm gs}\rangle \implies (E_{\rm gs} - H_d)\sum C_{S_d^z, s_{\rm tot}, s_{\rm tot}^z}|S_d^z, s_{\rm tot}, s_{\rm tot}^z\rangle = V\sum C_{S_d^z, s_{\rm tot}, s_{\rm tot}^z}|S_d^z, s_{\rm tot}, s_{\rm tot}^z\rangle \tag{61}$$

$E_{\rm gs}$ is the ground state energy, and can be replaced by the star graph ground state energy if we remove the kinetic energy cost via normal ordering: $E_{\rm gs} = -\frac{J}{2}\left(\frac{K}{2}+1\right)$. Since the interaction part V only changes $S_d^z \to -S_d^z$ and $s_{\rm tot}^z \to s_{\rm tot}^z \pm 1$, we can simplify the equation into individual smaller equations. For the two-channel model, the possible states are $(s_{\rm tot}, s_{\rm tot}^z) = (0,0),(1,-1),(1,0),(1,1)$. The individual equations for these states are

$$E_{\rm gs}|\frac{1}{2},1,0\rangle = \left(H_d + V\frac{1}{E_{\rm gs}-H_d}V^\dagger\right)|\frac{1}{2},1,0\rangle \tag{62}$$

$$E_{\rm gs}|-\frac{1}{2},1,0\rangle = \left(H_d + V^\dagger\frac{1}{E_{\rm gs}-H_d}V\right)|-\frac{1}{2},1,0\rangle \tag{63}$$

$$\tag{64}$$

These equations represent the Schrodinger equation for the states $|S_d^z,1,0\rangle$, and the right hand sides therefore give the effective Hamiltonians for those states. If we combine the states into a single subspace $|1,0\rangle = \left\{|\frac{1}{2},1,0\rangle, |-\frac{1}{2},1,0\rangle\right\}$, the effective Hamiltonian for this composite subspace becomes the sum of the two parts:

$$H_{\rm eff}^{1,0}|1,0\rangle\langle 1,0| = \left(H_d + VG_0V^\dagger + V^\dagger G_0 V\right)|1,0\rangle \tag{65}$$

where $G_0 = (E_{\rm gs} - H_d)^{-1}$. If we expand the subspace as $|1,0\rangle = |\frac{1}{2},1,0\rangle + |-\frac{1}{2},1,0\rangle$, we recover eqs. 62. Solving similarly for the other states gives

$$H_{\rm eff}^{1,1}|1,1\rangle\langle 1,1| = \left(H_d + V^\dagger G_0 V\right)|1,1\rangle \tag{66}$$

$$H_{\rm eff}^{1,-1}|1,-1\rangle\langle 1,-1| = \left(H_d + VG_0V^\dagger\right)|1,-1\rangle \tag{67}$$

To calculate these effective Hamiltonians, we will calculate the individual terms. We can easily simplify the S_d^z in the denominator of G_0, because $S_d^\pm \frac{1}{A+BS_d^z} = S_d^\pm \frac{1}{A\mp\frac{1}{2}B}$:

$$VG_0V^\dagger = \frac{J^2}{4}s_{\rm tot}^-\frac{\frac{1}{2}+S_d^z}{E_{\rm gs}+\frac{J}{2}s_{\rm tot}^z - H_0}s_{\rm tot}^+ \tag{68}$$

$$V^\dagger G_0 V = \frac{J^2}{4}s_{\rm tot}^+\frac{\frac{1}{2}-S_d^z}{E_{\rm gs}-\frac{J}{2}s_{\rm tot}^z - H_0}s_{\rm tot}^- \tag{69}$$

Since H_0 does not commute with the spin operators, we will need to expand the denominator to make sense of this Hamiltonian.

$$VG_0V^\dagger = s_{\rm tot}^-\frac{1}{E_{\rm gs}+\frac{J}{2}s_{\rm tot}^z}\left[1 + \frac{1}{E_{\rm gs}+\frac{J}{2}s_{\rm tot}^z}H_0 + \frac{1}{E_{\rm gs}+\frac{J}{2}s_{\rm tot}^z}H_0\frac{1}{E_{\rm gs}+\frac{J}{2}s_{\rm tot}^z}H_0 + \dots\right]s_{\rm tot}^+ \tag{70}$$

$$V^\dagger G_0 V = s_{\rm tot}^+\frac{1}{E_{\rm gs}-\frac{J}{2}s_{\rm tot}^z}\left[1 + \frac{1}{E_{\rm gs}-\frac{J}{2}s_{\rm tot}^z}H_0 + \frac{1}{E_{\rm gs}-\frac{J}{2}s_{\rm tot}^z}H_0\frac{1}{E_{\rm gs}-\frac{J}{2}s_{\rm tot}^z}H_0 + \dots\right]s_{\rm tot}^- \tag{71}$$

This is an expansion in $H_0^n/J^{n+1}, n = 0,1,2,\dots$. Expanding up to $n=2$ and keeping at most two particle interaction terms, the effective Hamiltonians for these states are:

$$H_{\rm eff}^{1,1} = H_0 + JS_d^z + \frac{J^2}{4}\frac{2}{E_{\rm gs}}\left[1 + \frac{H_0}{E_{\rm gs}} + \frac{s_{\rm tot}^+ X_{1,\rm tot}}{2E_{\rm gs}} + \frac{H_0^2}{E_{\rm gs}^2} - \frac{Z_{1,\rm tot}H_0}{E_{\rm gs}^3}\right]\left(\frac{1}{2} - S_d^z\right) \tag{72}$$

$$H_{\rm eff}^{1,-1} = H_0 - JS_d^z + \frac{J^2}{4}\frac{2}{E_{\rm gs}}\left[1 + \frac{H_0}{E_{\rm gs}} - \frac{s_{\rm tot}^- X_{1,\rm tot}^\dagger}{2E_{\rm gs}} + \frac{H_0^2}{E_{\rm gs}^2} - \frac{Z_{1,\rm tot}H_0}{E_{\rm gs}^3}\right]\left(\frac{1}{2} + S_d^z\right) \tag{73}$$

$$H_{\rm eff}^{1,0} = H_0 + \frac{J^2}{2\left(E_{\rm gs}+\frac{J}{2}\right)}\left[1 + \frac{H_0 + \left(\frac{1}{2}+S_d^z\right)s_{\rm tot}^+ X_{1,\rm tot} - \left(\frac{1}{2}-S_d^z\right)s_{\rm tot}^- X_{1,\rm tot}^\dagger}{2\left(E_{\rm gs}+\frac{J}{2}\right)} + \frac{H_0^2}{\left(E_{\rm gs}+\frac{J}{2}\right)^2} - \frac{Z_{1,\rm tot}H_0}{\left(E_{\rm gs}+\frac{J}{2}\right)^3}\right] \tag{74}$$

We employed the definitions $X_{n,\text{tot}} \equiv \sum_l \sum_{k,k'} (\epsilon_k - \epsilon_{k'})^n c^\dagger_{k\downarrow} c_{k'\uparrow}, X_{n,l}$ and $Z_{1,\text{tot}} \equiv \sum_{k,k',l} (\epsilon_k - \epsilon_{k'}) \frac{1}{2} \left(c^\dagger_{k\uparrow,l} c_{k'\uparrow,l} - c^\dagger_{k\downarrow,l} c_{k'\downarrow,l} \right)$. Focusing on the effective Hamiltonian for $(1,0)$, we see lots of non-Fermi liquid terms of the form $s^+_{\text{tot}} X_{1,\text{tot}}, s^-_{\text{tot}} X^\dagger_{1,\text{tot}}, Z_{1,\text{tot}} H_0$. These arise because of the degenerate manifold and the increased availability of states in the Hilbert space for scattering, as compared to the unique singlet ground state of the single-channel Kondo model.

B. Local low-energy effective Hamiltonian

Here we start with the low energy zero mode fixed point Hamiltonian for the two-channel Kondo obtained under URG treatment. Our goal here is to add excitations on top of this ground state and using the perturbation theory. In doing so we consider the leading order scatter appearing in the lowest order in the perturbative expansion. Note, in the fixed point zero mode Hamiltonian impurity spin is coupled with the bath electrons via spin exchange coupling, there is no charge exchange coupling present.

$$H^{(2)} = \alpha \vec{S}_{imp}.(\vec{S}_1 + \vec{S}_2) \quad , \quad \vec{S}_i = \frac{1}{2}\, c^\dagger_{i,\alpha}\, \vec{\sigma}_{\alpha,\beta}\, c_{i,\beta} \tag{75}$$

Here $\vec{S}_i = 1,2$ represents the spin degree of freedom present in the origin of the i^{th} channel. Thus one can rewrite the Eq.(75) interms of the electronic degree of freedom as,

$$\begin{aligned}\mathcal{H}_0 &= H_{0_1} + H_{0_2} \\ &= \alpha S^z_{imp}.\left(\frac{n_{1,\uparrow} - n_{1,\downarrow}}{2}\right) + \frac{1}{2}\left(S^+_{imp} c^\dagger_{1,\downarrow} c_{1,\uparrow} - S^-_{imp} c^\dagger_{1,\uparrow} c_{1,\downarrow}\right) \\ &+ \alpha S^z_{imp}.\left(\frac{n_{2,\uparrow} - n_{2,\downarrow}}{2}\right) + \frac{1}{2}\left(S^+_{imp} c^\dagger_{2,\downarrow} c_{2,\uparrow} - S^-_{imp} c^\dagger_{2,\uparrow} c_{2,\downarrow}\right)\end{aligned} \tag{76}$$

Here the basis we are interested in is $\{\mathcal{B}\} = \{|S^z_{imp}, n_{1,\uparrow}, n_{1,\downarrow}, n_{2,\uparrow}, n_{2,\downarrow}\rangle\}$. In this basis we write down all $2^3 = 8$ states of the spin Hamiltonian eq.(75)

$$\begin{aligned}|\alpha_0\rangle &= \frac{1}{\sqrt{6}}\Big[2|\Downarrow,1,0,1,0\rangle - |\Uparrow,0,1,1,0\rangle - |\Uparrow,1,0,0,1\rangle\Big] \\ |\alpha_1\rangle &= \frac{1}{\sqrt{6}}\Big[2|\Uparrow,0,1,0,1\rangle - |\Downarrow,1,0,0,1\rangle - |\Downarrow,0,1,1,0\rangle\Big] \\ E_{\alpha_0} &= E_{\alpha_1} = -\alpha\end{aligned} \tag{77}$$

$$\begin{aligned}|\beta_0\rangle &= \frac{1}{\sqrt{2}}\Big[|\Downarrow,1,0,0,1\rangle - |\Downarrow,0,1,1,0\rangle\Big] \\ |\beta_1\rangle &= \frac{1}{\sqrt{2}}\Big[|\Uparrow,1,0,0,1\rangle - |\Uparrow,0,1,1,0\rangle\Big] \\ E_{\beta_1} &= E_{\beta_2} = 0\end{aligned} \tag{78}$$

$$\begin{aligned}|\gamma_0\rangle &= \frac{1}{\sqrt{3}}\Big[|\Uparrow,0,1,0,1\rangle + |\Downarrow,1,0,0,1\rangle + |\Downarrow,0,1,1,0\rangle\Big] \\ |\gamma_1\rangle &= \frac{1}{\sqrt{3}}\Big[|\Uparrow,1,0,0,1\rangle + |\Uparrow,0,1,1,0\rangle + |\Downarrow,1,0,1,0\rangle\Big] \\ |\gamma_2\rangle &= |\Uparrow,1,0,1,0\rangle \\ |\gamma_3\rangle &= |\Downarrow,0,1,0,1\rangle \\ E_{\gamma_0} &= E_{\gamma_1} = E_{\gamma_2} = E_{\gamma_3} = \frac{\alpha}{2}\end{aligned} \tag{79, 80}$$

Note this spin Hamiltonian has total 8 states, where ground state is double degenerate with energy $-\alpha$ and the lowest exicites state with energy 0 is also double degenerate and the second excited state with energy $\alpha/2$ is 4-fold degenerate.

On top of the zero mode spin-channel interactions we want to consider the effect of the momentum space kinetic energy term $\sum_k \epsilon_k (n_{1,k} + n_{2,k})$. We assume identical dispersion for both the channels. Our zero mode spin Hamiltonian is written in the real space, thus it will be easier to do the perterbation theory on the real space. The fourier transformation of the momentum space kinetic energy term leads to real space hopping term. For simplicity we will be considering the neareast neighbor hoppings between sites within each channels. The real space hopping contributino to the Hamiltonian H_X with the hooping strength is

$$H_X = -t \sum_{\substack{<1,l_1> \\ <2,l_2>}} (c^\dagger_{1,\sigma} c_{l_1,\sigma} + c^\dagger_{2,\sigma} c_{l_2,\sigma} + \text{ h.c.}) \tag{81}$$

Here l_i represents the nearest site to the origin of the i^{th} channel. Thus here we are interested in studying the Hamiltonian $\mathcal{H}_0 + H_X$. The perterbating term H_x contains scattering which takes the states of the zero mode Hamltonain out of spin-channel scattering space. Thus befor we start the perturbation theroy we must expand the basis of the zero mode Hamiltonian itself. Thus the basis which contains the nearest neighbor sites of both the channels is given as

$$\begin{aligned}\{\mathcal{B}_{extnd}\} &\equiv \{\mathcal{B}\} \otimes \{|n_{l_1,\uparrow}, n_{l_1,\downarrow}, n_{l_2,\uparrow}, n_{l_2,\downarrow}\rangle\} \\ &= \{|S^z_{imp}, n_{1,\uparrow}, n_{1,\downarrow}, n_{2,\uparrow}, n_{2,\downarrow}\rangle \otimes |n_{l_1,\uparrow}, n_{l_1,\downarrow}, n_{l_2,\uparrow}, n_{l_2,\downarrow}\rangle\}\end{aligned} \tag{82}$$

Note there are $2^4 = 16$ elements in the subspace $\{|n_{l_1,\uparrow}, n_{l_1,\downarrow}, n_{l_2,\uparrow}, n_{l_2,\downarrow}\rangle\}$. In the spin-channel basis $\{\mathcal{B}\}$ there 2 degenerate ground states. Because the unpurterbed Hamiltonian $\mathcal{H}_0$ has no scattering terms outside the spin sector, in the extended basis $\{\mathcal{B}_{extnd}\}$ the total ground state deneracy becomes simply 2×2^4, 32 fold. Thus the total hamiltonian we are interested in is

$$\begin{aligned}\mathcal{H} = \frac{\alpha\hbar}{2}\, \vec{S}_d. \sum_{i=\{1,2\}} \sum_{\alpha,\beta\in\{\uparrow,\downarrow\}} c^\dagger_{i\alpha} \vec{\sigma}_{\alpha\beta} c_{i\alpha} \\ - t \sum_{i=\{1,2\}} \sum_{\substack{\langle i,l_i\rangle \\ \sigma}} (c^\dagger_{i,\sigma} c_{l_i,\sigma} + \text{h.c.})\end{aligned} \tag{83}$$

There are two degenrate states $|\alpha_1\rangle$ and $|\alpha_2\rangle$. Thus the two degenerate ground states in the above basis is give as,

$$|\tilde{\alpha}_0\rangle = |\alpha_0\rangle \otimes |n_{l_1,\uparrow}, n_{l_1,\downarrow}, n_{l_2,\uparrow}, n_{l_2,\downarrow}\rangle \tag{84}$$

$$|\tilde{\alpha}_1\rangle = |\alpha_1\rangle \otimes |n_{l_1,\uparrow}, n_{l_1,\downarrow}, n_{l_2,\uparrow}, n_{l_2,\downarrow}\rangle \tag{85}$$

Using degenerate perturbation theory we calculate the first and the second order corrections to the Hamiltonian. The first order and the second order low energy effective Hamiltonian is given as

$$\begin{aligned} H^{(1)} &= \sum_{ij} |\alpha_i\rangle\langle\alpha_i|V|\alpha_j\rangle\langle\alpha_j| \\ H^{(2)} &= \sum_{ij}\sum_{l} |\alpha_i\rangle \frac{\langle\alpha_i|V|\mu_l\rangle\langle\mu_l|V|\alpha_j\rangle}{E_0 - E_l}\langle\alpha_j| \end{aligned} \tag{86}$$

where $|\alpha_i\rangle$ represents the ground states with energy E_0 and μ_l represents the ecvited states with energy E_l. One can easily check the diagonal term in effective Hamiltonain coming from the 1^{st} or any *odd* order correction is zero as the state never returns to the original starting state via odd number of scatterings. For the case of first order it is easy to see that the off-diagonal correction to the effective Hamiltonian is also zero. Thus the lowest order where we expect the non-zero corrections is the second order. We first calculate the diagonal correction in the first order

$$H^{(2)}_{diag} = \sum_{i}\sum_{l} |\alpha_i\rangle\langle\alpha_i| \frac{|\langle\alpha_i|V|\mu_l\rangle|^2}{E_0 - E_l} \tag{87}$$

As single scattering always takes the state outside of the spin-channel, the state $V|\alpha_i\rangle$ is an excited state with energy 0 ($= E_l$). This α_i representing the ground state can take total 32 configurations as discussed. Out of this 32 states $|\alpha_0\rangle\otimes|n_{l_1,\uparrow}, n_{l_1,\downarrow}, n_{l_2,\uparrow}, n_{l_2,\downarrow}\rangle$ can take 16 configurations and $|\alpha_1\rangle \otimes |n_{l_1,\uparrow}, n_{l_1,\downarrow}, n_{l_2,\uparrow}, n_{l_2,\downarrow}\rangle$ can take the rest 16 configurations. Note the two degnereate states $|\tilde{\alpha}_0\rangle$ and $|\tilde{\alpha}_1\rangle$ is labeled by the J^z eigenvalue $\pm 1/2$ respectively, where J^z is the total z-component of the impurity and zero modes of the baths. Thus these 32 ground states can be seperated in two 16 state groups labeled by the $J^z = \pm 1/2$ eigenvalues. For the $J^z = 1/2$ sector we get the effective Hamiltonian

$$H^{(2)}_{diag}(1/2) = \frac{2t^2}{E_0}\hat{I} - \frac{2t^2}{3E_0}\Big[(n_{l_1\uparrow} - n_{l_1\downarrow}) + (n_{l_2\uparrow} - n_{l_2\downarrow})\Big] \tag{88}$$

Similarly the for $J^z = -1/2$ we get

$$H^{(2)}_{diag}(1/2) = \frac{2t^2}{E_0}\hat{I} + \frac{2t^2}{3E_0}\Big[(n_{l_1\uparrow} - n_{l_1\downarrow}) + (n_{l_2\uparrow} - n_{l_2\downarrow})\Big] \tag{89}$$

Thus the diagonal part of the effective Hamiltonian in the second order is

$$\begin{aligned} H^{(2)}_{diag} &= \sum_{i}\sum_{l} |\alpha_i\rangle\langle\alpha_i| \frac{|\langle\alpha_i|V|\mu_l\rangle|^2}{E_0 - E_l} \\ &= -4t^2\hat{I} \end{aligned} \tag{90}$$

where $\hat{I}$ is the identity operator made out of all $2^4 = 16$ possible number operator combinations as shown below

$$\hat{I} = \sum_{\hat{o}=\hat{n},(1-\hat{n})} \hat{o}_{l_1,\uparrow}\hat{o}_{l_1,\downarrow}\hat{o}_{l_2,\uparrow}\hat{o}_{l_2,\downarrow} \tag{91}$$

Now we are interested in calcualting the offdiagonal term present in the second order low energy effective Hamiltonian which is given as

$$\begin{aligned} H^{(2)}_{off} &= \sum_{i\neq j}\sum_{l} |\alpha_i\rangle \frac{\langle\alpha_i|V|\mu_l\rangle\langle\mu_l|V|\alpha_j\rangle}{E_0 - E_l}\langle\alpha_j| \\ &= -\frac{8t^2}{3}\Big[(S^z_1)^2 c^\dagger_{2\uparrow}c_{2\downarrow}\Big(c_{l_1\uparrow}c^\dagger_{l_1\downarrow} + c_{l_2\uparrow}c^\dagger_{l_2\downarrow}\Big) \\ &+ (S^z_2)^2 c^\dagger_{1\uparrow}c_{1\downarrow}\Big(c_{l_1\uparrow}c^\dagger_{l_1\downarrow} + c_{l_2\uparrow}c^\dagger_{l_2\downarrow}\Big)\Big] + \text{h.c.} \end{aligned} \tag{92}$$

C. Studying the LEH

1. *Self energy and Specific heat*

Here we study this LEH to understant valrious features like change in the self-energy, and the nature of the momentum space Hamiltonian. To calculate the self energy we fo Hartee-Fock to get the shift in the kinetic energy. In the real space one can get a diagonal piece from the above equation by using the Fermionic anticommutation relations.

$$H^{off,(2)}_{eff}|_{diag} = -\frac{16t^2}{3}[(S^z_1)^2 + (S^z_2)^2] \tag{93}$$

We can find the corresponding momentum space Hamiltonian by doing the fouries transforamtion to the Hamiltonian $H^{off,(2)}_{eff}|_{diag}$.

$$\begin{aligned} H^{off,(2)}_{eff}|_{diag} = -\frac{4t^2}{3}\frac{1}{N}\Big[\sum_{k,\sigma} n_{k\sigma}\Big(1 - \frac{1}{N}\sum_{k_2} n_{k_2,-\sigma}\Big) \\ + \sum_{k,\sigma}\tilde{n}_{k\sigma}\Big(1 - \frac{1}{N}\sum_{k_2}\tilde{n}_{k_2,-\sigma}\Big)\Big] \end{aligned} \tag{94}$$

in momentum space we can do again the Hartee-Fock to measure the self-energy

$$\begin{aligned} \bar{\epsilon}_k - \epsilon_k = \Sigma_k &= -\frac{4t^2}{3N}\Big(1 - \frac{1}{N}\sum_{k_2}\langle n_{k_2,-\sigma}\rangle\Big) \\ &= -\frac{4t^2}{3N^2}\Big(1 - \frac{N}{e^{(\epsilon_k-\mu)/k_BT} + 1}\Big) \end{aligned} \tag{95}$$

Using the self-energy we calculate the impurity speciftic heat defined as $C_{imp} = C(J^*) - C(0)$.

$$C_{imp} = \sum_{\Lambda,\sigma}\beta\Big[\frac{(\bar{\epsilon}_\Lambda)^2 e^{\beta\bar{\epsilon}_\Lambda}}{(e^{\beta\bar{\epsilon}_\Lambda} + 1)^2} - \frac{(\epsilon_\Lambda)^2 e^{\beta\epsilon_\Lambda}}{(e^{\beta\epsilon_\Lambda} + 1)^2}\Big] \tag{96}$$

Here we are intersted in the low temperature behavior of this impurity specific-heat. Using the self-energy obtained above we calculate the impurity susecptibility for

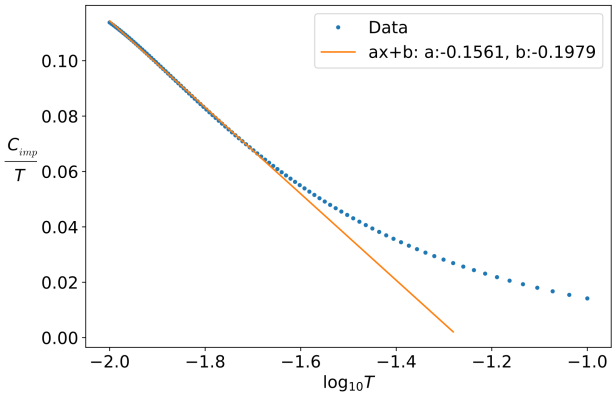

FIG. 14. This figure shows the variation of the impurity specific heat with the temperature.

$t = 0.1$ and $\alpha = 1$. The above Fig.14 shows that at low temperature follows logarithmic behavior for the single channel case which is in agreement with the results known in the literature [CITE].

$$\frac{C_{imp}}{T} \propto \log T \tag{97}$$

2. *Exact diagonalization*

Here we do the exact diagonalization the NFL Hamiltonian eq.(92) and find the eigenspectrum. Using this eigen spectrum we computer various quantitites like χ. We can compute other quantities from this exact diagonalization.

$$\chi = \beta\left[\frac{\sum e^{-\beta\bar{\epsilon}_\Lambda}\langle\bar{S}^{z2}\rangle}{\sum e^{-\beta\bar{\epsilon}_\Lambda}} - \frac{\sum e^{-\beta\epsilon_\Lambda}\langle S^{z2}\rangle}{\sum e^{-\beta\epsilon_\Lambda}}\right] \tag{98}$$

We numerically compute the χ from the definition above and study it's dependence on temperature. The above figure shows that at low temperture

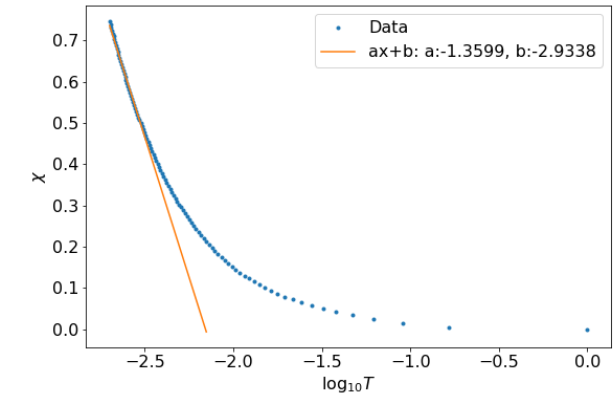

$$\chi(T) \propto \log T \tag{99}$$

This matches with the already known result of the literature. The ratio $\frac{\chi(T)}{C_{imp}/T} \sim 8.3$ greater than the Wilson ration. One can check this quantity for larger system size and at lower temperature for an better agreement.

3. *Momentum space structure of the NFL*

Direct fourier transformation on the $H^{(2)}_{off}$ leads to the LEH in momentum space showing higher order scattering involving electronic degree of freedoms. The Fourier transformation of the electronic creation operator gives

Thus one gets,

$$\begin{aligned}(S^z_1)^2\Big|_{diag} &= \frac{1}{4}(n_{1\uparrow}-n_{1\downarrow})^2\Big|_{diag} = (n_{1\uparrow}+n_{1\downarrow}-2n_{1\uparrow}n_{1\downarrow})/4\Big|_{diag} \\ &= \frac{1}{4N}\sum_{k,\sigma} n_{k\sigma} - \frac{1}{4N^2}\sum_{k_1,k_2,\sigma} n_{k_1,\sigma}n_{k_2,-\sigma}\end{aligned} \tag{100}$$

We know that the diagoanl peice of the following terms is given as

Thus the diagonal piece coming from the term,

$$c^\dagger_{2\uparrow}c_{2\downarrow}\left(c_{l_1\uparrow}c^\dagger_{l_1\downarrow} + c_{l_2\uparrow}c^\dagger_{l_2\downarrow}\right) \Rightarrow \frac{1}{N}\sum_{k,k'} e^{-i(k-k')r}c^\dagger_{k,\sigma}c_{k',-\sigma}$$

Thus we get the diagonal correction of effective Hamiltonian in the momoentum spcae,

$$H_{eff}^{off,(2)}\Big|_{diag} = -\frac{8t^2}{3}\left[\frac{1}{4N}\sum_{k,\sigma} n_{k\sigma} - \frac{1}{2N^2}\sum_{k_1,k_2} n_{k_1\uparrow} n_{k_2\downarrow}\right] \times \left[\frac{1}{N^2}\sum_{k_1,k_2} \tilde{n}_{k_1\uparrow}(1-\tilde{n}_{k_2\downarrow}) + (\uparrow\to\downarrow)\right] \times 2$$
$$= -\frac{4t^2}{3}\left[\frac{1}{N}\sum_{k,\sigma} n_{k\sigma} - \frac{1}{N^2}\sum_{k_1,k_2,\sigma} n_{k_1,\sigma} n_{k_2,-\sigma}\right] \times \left[\frac{1}{N}\sum_{k_1,\sigma} \tilde{n}_{k_1,\sigma} - \frac{1}{N^2}\sum_{k_1,k_2,\sigma} \tilde{n}_{k_1\sigma}\tilde{n}_{k_2,-\sigma}\right], \quad (101)$$

Where $n_{k,\sigma}$ and $\tilde{n}_{k,\sigma}$ are the occupation of the states k,σ corresponding to two different channels. One can define the charge density of i^{th} channel with the spin-σ as

$$q_{i,\sigma} = \frac{Q_{i,\sigma}}{N} = \frac{1}{N}\sum_k n_{k,\sigma} \quad (102)$$

Thus one can re-write the abeove equation as,

$$H_{eff}^{off,(2)}\Big|_{diag} = -\frac{4t^2}{3}\prod_{i=\{1,2\}}\left[q_{i,\uparrow} + q_{i,\downarrow} - q_{i,\uparrow}q_{i,\downarrow}\right] \quad (103)$$

This shows the inter-channel charge coupling present in the excitation spectrum.

D. Third order

Thus the off-diagonal part of the effective low energy Hamiltonian in the 2nd order is

$$H_{eff,off}^{(2)} = \frac{J^2}{\alpha}\Bigg[c_{1\uparrow}c_{1\downarrow}^\dagger\Bigg(-\alpha\beta\Big\{\Sigma_{3,2} + c_{3\uparrow}^\dagger c_{3\downarrow} c_{2\uparrow} c_{2\downarrow}^\dagger\Big\} - \alpha\gamma\Omega_{3,2}\Bigg)$$
$$+ c_{2\uparrow}c_{2\downarrow}^\dagger\Bigg(-\alpha\beta\Big\{\Sigma_{1,3} + c_{1\uparrow}^\dagger c_{1\downarrow} c_{3\uparrow} c_{3\downarrow}^\dagger\Big\} - \alpha\gamma\Omega_{1,3}\Bigg)$$
$$+ c_{3\uparrow}c_{3\downarrow}^\dagger\Bigg(-\alpha\beta\Big\{\Sigma_{2,1} + c_{2\uparrow}^\dagger c_{2\downarrow} c_{1\uparrow} c_{1\downarrow}^\dagger\Big\} - \alpha\gamma\Omega_{2,1}\Bigg) + \text{h.c.}\Bigg]$$
$$\otimes\Big[c_{l_1\uparrow}^\dagger c_{l_1\downarrow} + c_{l_2\uparrow}^\dagger c_{l_2\downarrow} + c_{l_3\uparrow}^\dagger c_{l_3\downarrow} + \text{h.c.}\Big]$$

$$\Sigma_{i,j} = -8S_i^z S_j^z[(C_i^z - C_j^z)^2 + (S_i^z - S_j^z)^2] \quad (104)$$
$$\Omega_{i,j} = 4S_i^z S_j^z(C_i^z + C_i^z)(C_j^z + C_j^z) \quad (105)$$

Now we are interested calculating the diagonal part of the effective Hamiltonian. In this case we get non-zero contribution from all the three ground states $|J^z=-1\rangle$, $|J^z=0\rangle$ and $|J^z=1\rangle$. We get the diagonal contribution to the LEH in the second order is

$$H_{eff,diag}^{(2)} = -\frac{7.2J^2}{\alpha}\hat{I} \quad (106)$$

The contribution associater to different ground states $|J^z=-1\rangle$, $|J^z=0\rangle$ and $|J^z=1\rangle$ is given respectively as $-\frac{2.4J^2}{\alpha}\hat{I}+\hat{\mathcal{F}}, -\frac{2.4J^2}{\alpha}\hat{I}, -\frac{2.4J^2}{\alpha}\hat{I}-\hat{\mathcal{F}}$, where $\hat{\mathcal{F}}$ is a function of diagonal number oprators of the nearest-neighbor site degree of freedom l_1, l_2, l_3 etc.

E. Presence of a marginal Fermi liquid: Orthogonality catastrophe in two-channel MCK model

At the stable fixed point $J^* = J_1^* = \frac{2}{K\rho}$, the ground states of the Hamiltonian are those of the star graph model, with a degeneracy of K. We now specialise to the two-channel Kondo model. To find the low-energy excitations on top of this ground state manifold, we insert a tight-binding nearest-neighbour hopping between the zeroth site (the one that holds the impurity) and the first site (site that's nearest to the zeroth site) as a perturbation and calculate the diagonal and off-diagonal terms generated by this perturbation. It is found that when we trace out the impurity, we are left only with real space off-diagonal terms:

$$V_{\text{eff}} = \frac{2t^2}{J^*}\left[\left(\sigma_{0,1}^z\right)^2 s_{0,2}^+ + \left(\sigma_{0,2}^z\right)^2 s_{0,1}^+\right]\left(s_{1,1}^- + s_{1,2}^-\right) + \text{h.c.} \quad (107)$$

where $\sigma_{0,l}^z = \hat{n}_{0\uparrow,l} - \hat{n}_{0\downarrow,l}$, $s^+ = c_{0\uparrow,l}^\dagger c_{0\downarrow,l}$ and $s^- = (s^+)^\dagger$. The notation $0\sigma, l$ has the site index $i = 0, 1, 2, \ldots$ as the first label, the spin index $\sigma = \uparrow, \downarrow$ as the second label and the channel index $l = 1, 2$ as the third index.

These are the terms that are generated because of the presence of the impurity. Such a non-Fermi liquid (NFL) contribution to the effective Hamiltonian and the absence of any Fermi-liquid term at the same order should be contrasted with the local Fermi liquid excitations induced by the singlet ground state of the single-channel Kondo model [29, 45, 52]. We wish to point out that such NFL terms were also obtained by Coleman, et al. [39] in terms of Majorana fermions at the zeroth site and the first site of the $\sigma - \tau$ version of the two-channel Kondo model. They then went on to compute a single-particle self-energy renormalisation coming from this NFL term that matches the phenomenological [53] and microscopic forms of the marginal Fermi liquid self-energy [3, 54]. We take a different route in order to calculate the self-energy contribution coming from Eq. 107.

In the URG analysis of the 2D Hubbard model at half-filling [3], it was found that the normal phase of the Mott insulator was a metal with properties that have been phenomenologically attributed to the marginal Fermi liquid. The excitations of such a phase are described by a two particle-one hole composite object:

$$H_{\text{MFL}} = \sum_{k,k',k'',\sigma} R\hat{n}_{k\sigma}\hat{n}_{k'\overline{\sigma}}\left(1 - \hat{n}_{k''\sigma}\right) \quad (108)$$

We wish to look for such a term in the effective Hamiltonian. For this, we will perform a perturbative treatment of the hopping at strong coupling $J \to \infty$ where the perturbative coupling t^2/J is arbitrarily small and again obtain Eq. 107. Such a change from the strong coupling model with parameter J to a weak coupling model with parameter t^2/J amounts to a duality transformation [31, 32]. It can be shown that the duality transformation leads to an identical MCK model [31] (self-duality), which implies we can have identical RG flows, and our transformation simply extracts the NFL piece from the dual model. The self-duality also ensures that the critical intermediate-coupling fixed point is unique and can be reached from either of the models.

The diagonal part of eq. 107 is

$$V_{\text{eff}} = \frac{2t^2}{J} \sum_{l=1,2} \left(\sum_{\sigma} \hat{n}_{0\sigma,l} \right) s^{+}_{0,\bar{l}} s^{-}_{1,\bar{l}} + \text{h.c.} \tag{109}$$

where $\bar{l} = 3 - l$ is the channel index complementary to l. We will fourier transform this effective Hamiltonian into $k-$space. The NFL part becomes

$$\sum_{\sigma,\{k_i,k_i'\},l} \frac{2t^2}{J} e^{i(k_1-k_1')a} c^{\dagger}_{k\sigma,l} c_{k'\sigma,l} c^{\dagger}_{k_2\uparrow,\bar{l}} c_{k_2'\downarrow,\bar{l}} c^{\dagger}_{k_1\downarrow,\bar{l}} c_{k_1'\uparrow,\bar{l}} + \text{h.c.} \tag{110}$$

This form of the Hamiltonian is very similar to the three-particle interaction term in Appendix B of [54]. The channel indices in Eq. 110 can be mapped to the normal directions in [54]. As specualted eariler, the 2 particle-1 hole interaction in Eq. 110 has a diagonal component which can be obtained by setting $k = k', k_1 = k_2'$ and $k_2 = k_1'$:

$$\begin{aligned} H_{\text{eff,MFL}} &= \sum_{\substack{k,k_1,\\ k_2,\sigma,l}} \frac{2t^2 e^{i(k_1-k_2)a}}{J} \hat{n}_{k\sigma,l} \hat{n}_{k_2\uparrow,\bar{l}} \left(1 - \hat{n}_{k_1\downarrow,\bar{l}}\right) + \text{h.c.} \\ &= \sum_{\substack{k,k_1,\\ k_2,\sigma,l}} \frac{4t^2}{J} \cos a\,(k_1 - k_2)\, \hat{n}_{k\sigma,l} \hat{n}_{k_2\uparrow,\bar{l}} \left(1 - \hat{n}_{k_1\downarrow,\bar{l}}\right) \end{aligned} \tag{111}$$

The most dominant contribution comes from $k_1 = k_2 = k'$, revealing the non-Fermi liquid metal [15, 38]:

$$H^{*}_{\text{eff,MFL}} = \frac{4t^2}{J} \sum_{\sigma,k,k',l} \hat{n}_{k\sigma,l} \hat{n}_{k'\uparrow,\bar{l}} \left(1 - \hat{n}_{k'\downarrow,\bar{l}}\right) \tag{112}$$

Following [54], one can follow the RG evolution of the dual coupling $R_j = \frac{4t^2}{J_j}$ at the j^{rh} RG step, in the form of the URG equation

$$\Delta R_j = -\frac{R_j^2}{\omega - \epsilon_j/2 - R_j/8} \tag{113}$$

In the RG equation, ϵ_j represents the energy of the j^{th} isoenergetic shell. It is seen from the RG equation that R is relevant in the range of $\omega < \frac{1}{2}\epsilon_j$ that has been used throughout, leading to a fixed-point at $R^*/8 = \omega - \frac{1}{2}\epsilon^*$). The relevance of R is expected because the strong coupling J is irrelevant and $R \sim 1/J$.

The renormalisation in R leads to a renormalisation in the single-particle self-energy [54]. The $k-$space-averaged self-energy renormalisation is

$$\Delta\Sigma(\omega) = \rho R^{*2} \int_0^{\epsilon^*} \frac{d\epsilon_j}{\omega - \epsilon_j/2 + R_j/8} \tag{114}$$

The density of states can be approximated to be N^*/R^*, where N^* is the total number of states over the interval R^*. As suggested by the fixed point value of R_j, we can approximate its behaviour near the fixed point by a linear dependence of the dispersion ϵ_j. The two limits of the integration are the start and end points of the RG. We start the RG very close to the Fermi surface and move towards the fixed point ϵ^*. Near the start point, we substitute $\epsilon = 0$ and $R = \omega$, following the fixed point condition. From the the fixed point condition, we also substitute $R^*/8 = \omega - \frac{1}{2}\epsilon^*$. On defining $\bar{\omega} = N^* \left(\omega - \frac{1}{2}\epsilon^*\right)$, we can write

$$\Delta\Sigma(\omega) \sim \bar{\omega} \ln \frac{N^*\omega}{\bar{\omega}} \tag{115}$$

The self-energy also provides the quasiparticle residue for each channel[54]:

$$Z(\bar{\omega}) = \left(2 - \ln \frac{2\bar{\omega}}{N^*\omega}\right)^{-1} \tag{116}$$

As the energy scale $\omega \to 0$, the Z vanishes, implying that the ground state and lowest-lying excitations, in the presence of the NFL terms, are not adiabatically connected to the Fermi gas. This is the orthogonality catastrophe [53, 55–57] in the two-channel Kondo problem, and it is brought about by the presence of the terms in Eq. 112. Such terms were absent in the single-channel Kondo model, because there was no multiply-degenerate ground state manifold that allowed scattering. This line of argument shows that the extra degeneracy of the ground state subspace and the frustration of the singlet order that comes about when one upgrades from the single-channel Kondo model to the MCK models is at the heart of the NFL behaviour, and the orthogonality catastrophe should be a general feature of all such frustrated MCK models. A local NFL term with a self-energy of the form in eq. 115 was also obtained in the $\sigma - \tau$ model by Coleman et al. [39]. The common features show the universality between the two-channel Kondo and the $\sigma - \tau$ models.

V. LOCAL MOTT LIQUID

Using the unitary renormalization group method we decouple the impurity spin from the zero-modes of the K

channels. We start with the Hamiltonian. The zero mode Hamiltonian is a stargraph model

$$H = \alpha \vec{S}_d . \sum_i \vec{S}_i = \alpha S_d^z S^z + \frac{\alpha}{2}(S_d^+ S^- + S_d^- S^+)$$
$$H_D = \alpha S_d^z S^z \ , \quad H_X = \frac{\alpha}{2}(S_d^+ S^- + S_d^- S^+) \tag{117}$$

Here we want to remove the quantum fluctuations between the impurity spin and the rest, for that we do one step URG.

$$\Delta H = H_X \frac{1}{\hat{\omega} - H_D} H_X \tag{118}$$

In the zero mode IR fixed point ground state (star graph) of multi-channel ground state J^z is a good quantum number but S^z is not. There is no net S^z field thus in the ground state manifold the average S^z is vanishing, $\langle S^z \rangle = 0$. We use this expectation value to replace the denominator of the above RG equation.

Thus we get the effective Hamiltonian is

$$\begin{aligned} H_{eff} &= \frac{\alpha^2 \Gamma_\uparrow}{2}(S^2 - S^{z2})(\tau_d^2 - \tau_d^z) \\ &= \beta_\uparrow(\alpha, \omega_\uparrow)(S^2 - S^{z2})(\tau_d^2 - \tau_d^z) \ , \quad \frac{\alpha^2 \Gamma_\uparrow}{2} = \beta_\uparrow(\alpha, \omega_\uparrow) \\ &= \frac{\beta_\uparrow(\alpha, \omega_\uparrow)}{2}(S^2 - S^{z2}) = \frac{\beta_\uparrow(\alpha, \omega_\uparrow)}{4}(S^+ S^- + S^- S^+) \end{aligned} \tag{119}$$

. In terms of the electronics degree of freedom this looks

$$\begin{aligned} &H_{eff}(\omega, \alpha) \\ &= \frac{\beta_\uparrow(\alpha, \omega_\uparrow)}{4} \sum_{i \neq j} \sum_{\substack{\alpha_i, \beta_i \in \{\uparrow, \downarrow\} \\ \alpha_j, \beta_j \in \{\uparrow, \downarrow\}}} \vec{\sigma}_{\alpha_i \beta_i} \vec{\sigma}_{\alpha_j \beta_j} c_{0\alpha_i}^{(i)\dagger} c_{0\beta_i}^{(i)} c_{0\alpha_j}^{(j)\dagger} c_{0\beta_j}^{(j)} \\ &+ \text{h.c.} \end{aligned} \tag{120}$$

We will study the two cases of the above effective Hamiltonian depending on the sign of the prefactor. The case $\frac{\beta_\uparrow(\alpha,\omega_\uparrow)}{2} > 0$ is the ferromagnetic case where in the ground state S takes the minimum value and S^z takes the possible maximum value. For an example, in the case of K channels the minimum value of S will be 0 or 1/2 for K being *even* or *odd* respectively. We will be interested in the other case where $\frac{\beta_\uparrow(\alpha,\omega_\uparrow)}{2} < 0$. In this case the ground state corresponds to S being maximum and S^z being minimum case. The effective Hamiltonian can be re-written in this case as

$$H_{eff} = -\frac{|\beta_\uparrow(\alpha, \omega_\uparrow)|}{4}(S^+ S^- + S^- S^+) \tag{121}$$

The CSCO of this Hamiltonian contains H, S, S^z. In the ground state S is maximum thus $S = K/2$ and S^z can take $2S + 1 = K + 1$ values. Thus in the largest S sector there are $K + 1$ states. One can explore different states via a flux tuning mechanism. In the presence of the flux the Hamiltonian looks like

$$H = -\frac{|\beta_\uparrow(\alpha, \omega_\uparrow)|}{2} S^2 + \frac{|\beta_\uparrow(\alpha, \omega_\uparrow)|}{2}\left(S^z - \frac{\Phi}{\Phi_0}\right)^2 \tag{122}$$

A. Mapping with the degenerate ground state of stargraph

Now we are going to discuss about the mapping of K degenerate ground states of the parent $K-$channel stargraph model with the states of this flux-insterted all-to-all model obtained by removing inpurity-bath quantum fluctuations. In the stargraph model the K ground states is labeled by the J^z eigenvalues. In the stargraph ground state $J = S - 1/2$, where S is maximum with value $S = K/2$. Thus there are $2J + 1 = K$ unique J_z eigenvalues corresponding to the J sector labeling different eigenstates. The gound state Hilbert space $\mathcal{H}_{gr}$ contains the J^z states

$$\mathcal{H}_{gr} = \{-(K-1)/2, -(K-3)/2, \cdots, (K-3)/2, (K-1)/2\} \tag{123}$$

Now we shift our focus to the low energy Hamiltonian with flux shown in the eq.(122). We can see that there is a unique ground state labeled by the S^z eigenvalues. By tuning the flux (Φ/Φ_0) one can go from one ground state to another ground state or change the ground state. We can see that ground state energy is independent of the configuration of the impurity spin $(S_d^z = \pm 1/2)$. Thus for each of those two possibilities we get two set of ground states labeled by the S^z and the $J^z = S^z + S_d^z$. Similar to the stargraph case here also the ground state corresponds to the largest S sector, $S = K/2$. Thus total number of S^z eigenvalues are $2S + 1 = K + 1$ taking values $\{-K/2, -(K-2)/2, \cdots, (K-2)/2, K/2\}$.

$$\begin{aligned} S_d^z = +1/2 \ , \ \{J^z\} &= \{-(K-1)/2, -(K-3)/2, \cdots, (K-1)/2, (K+1)/2\} \\ S_d^z = -1/2 \ , \ \{J^z\} &= \{-(K+1)/2, -(K-1)/2, \cdots, (K-3)/2, (K-1)/2\} \end{aligned} \tag{124}$$

Thus one can see that the ground state degeneracy of the stargraph model with different J^z values gets lifted in the quantum fluctuation resolved all-to-all model. Depending on the value of the flux there is an unique ground state labeled by the J^z value. Tuning the fluc one can go from one ground state to the other. This shows how one can explore different degenerate ground states of the parent stargraph model via the insertion of flux in the

corresponding quantum fluctuation resolved all-to-all effective Hamiltonian.

B. Local mott-liquid

Impurity-bath quantum fluctuation resolved all-to-all effective Hamiltonian is written in terms of the spinor spin operators which are individually made out of two electronic degree of freedom. This is defined as $\vec{S}_i = \frac{\hbar}{2}\sum_{\alpha,\beta\in\{\uparrow,\downarrow\}} c^{(i)\dagger}_{0\alpha}\vec{\sigma}_{\alpha\beta}c^{(i)}_{0\beta}$. In the above eq.(120) we see the $U(1)$ symmetry of the effective Hamiltonian. Using the spinor repersentation one can see the spin creation operation in terms of the electronic degree of freedom is

$$S^+_i = \frac{\hbar}{2}\sum_{\alpha,\beta\in\{\uparrow\downarrow\}} c^{(i)\dagger}_{0\alpha}\sigma^+_{\alpha\beta}c^{(i)}_{0\beta} = \frac{\hbar}{2}c^{(i)\dagger}_{0\uparrow}c^{(i)}_{0\downarrow} \tag{125}$$

$$S^z_i = \frac{\hbar}{2}\sum_{\alpha,\beta\in\{\uparrow\downarrow\}} c^{(i)\dagger}_{0\alpha}\sigma^z_{\alpha\beta}c^{(i)}_{0\beta} = \frac{\hbar}{2}(c^{(i)\dagger}_{0\uparrow}c^{(i)}_{0\uparrow} - c^{(i)\dagger}_{0\downarrow}c^{(i)}_{0\downarrow}) \tag{126}$$

Thus this spinor spins are nothing but the Anderson pseudospin formulation in the spin channel. The spin creation opertor (S^+_i) shows simultaneous creation of an electron-hole pair at the realspace origin of the i^{th} channel. The condensation of such electron-hole pais has already been shown in [CITE: mott]. Thus for this effective Hamiltonian one can define twist-translation oeprations to construct the gauge theory and unveiling any hidden degeneracy. Let's recall the effective Hamiltonian

$$H_{eff} = \frac{\beta_\uparrow(\alpha,\omega_\uparrow)}{4}\left[\sum_{ij} S^+_i S^-_j \ + \text{h.c.}\right], \tag{127}$$

where i,j are the channel indices. Due to the all-to-all nature of the connectivity one can draw total $K!$ possible unique closed paths ($\mathcal{C}_\mu$) where each nodes (channels) is being touched only once. One can thus define total $K!$ number of translation operators ($\hat{T}_\mu$) which keeps the Hamiltonian invariant. Let's define one of such translation operator $\hat{T}_\mu$ thich gives a periodic shifts along the closed path $\mathcal{C}_\mu$. Let's define twist operator along the path $\mathcal{C}_\mu$

$$\hat{\mathcal{O}}_\mu = \exp(i\frac{2\pi}{K}\sum_{\substack{j=1\\ \mathcal{C}_\mu}}^{K} jS^z_j)\ , \quad \hat{T}_\mu = e^{i\hat{P}^{cm}_\mu} \tag{128}$$

The operation of the translation operator $\hat{T}_\mu$ is defined as $\hat{T}_\mu S^z_j = S^z_{j+1}$ where $j+1$ and j are the nearest neighbor on the closed path $\mathcal{C}_\mu$. Then the braiding rule between the twist and translation operators are give as

$$\begin{aligned}\hat{T}_\mu\hat{\mathcal{O}}_\mu\hat{T}^\dagger_\mu\hat{\mathcal{O}}^\dagger_\mu &= \exp\{i[2\pi S^z_1 - \frac{2\pi}{K}S^z]\}\\ &= \exp\{i[\pm\pi - \frac{2\pi}{K}S^z]\} = \exp(i\frac{2\pi p}{q})\end{aligned} \tag{129}$$

The availability of the non-trivial braiding staatistics between these twist and translation operators is possible if $p\neq 0$ and $q\neq\infty$. Further simplification leads to the condition

$$\begin{aligned}\pm\pi - \frac{2\pi}{K}S^z = \frac{2\pi p}{q} \quad &\Rightarrow \pm\frac{1}{2} - \frac{S^z}{K} = \frac{p}{q}\\ &\frac{(\pm K - 2S^z)}{2K} = \frac{p}{q}\ ,\end{aligned} \tag{130}$$

p,q are mutual prime, We knwo that the S^z can take values $(\mp K/2 \pm m)$ where m is a integer $0\leq m\leq K$. Putting this value in the above equation leads to two possible solutions.

$$\frac{(K-m)}{K} = \frac{p}{q}\ , \quad \frac{-m}{K} = \frac{p}{q} \tag{131}$$

For the first case $K-m=p$ we can see that $m=K$ makes p trivial hus the allowed values are $m=0,\cdots,K-1$, which represents the corresponding S^z eigen values

$$-K/2, -K/2+1, \cdots, K/2-2, K/2-1 \tag{132}$$

Similarly the second case implies, $-m=p$, but $p=0$ is not allowed as this makes the braiding statistics trivial, thus the possible S^z values are

$$-K/2+1, -K/2+2, \cdots, K/2-1, K/2 \tag{133}$$

Thus we get the general braiding statistics between the twist and the translation

$$\hat{T}_\mu\hat{\mathcal{O}}_\mu\hat{T}^\dagger_\mu{\hat{\mathcal{O}}_\mu}^\dagger = e^{i\frac{2\pi p}{K}} \tag{134}$$

where p corresponds to different S^z states, related as $p = \pm K/2 - S^z$. Thus we can see that there are K possible S^z plaleau states in the all-to-all model where each plateaux is K fold degenerate. This p/K is similar to the filling factor of the fractional quantum Hall effect. There are possibly $K!$ pairs of twist and translation operator corresponding to different closed paths $\mathcal{C}_\mu$ which can probe this degeneracy.

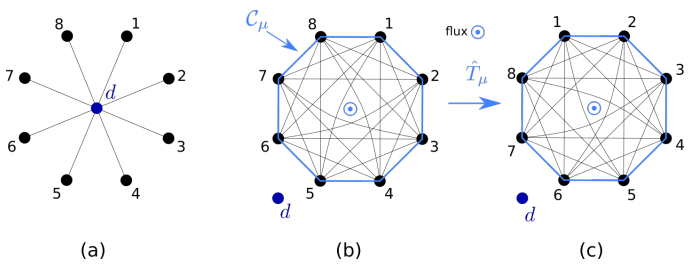

FIG. 15. This figure shows the comparison and mapping between the stargraph degenerate ground states and the states of the quantum fluctuation resolved all to all model.

1. Action on the Hamiltonian

Now we findout the action of these twist operators on the Hamiltonian. The Hamiltonian is written as

$$H_{eff} = \frac{\beta_\uparrow(\alpha,\omega_\uparrow)}{2}(S^{x2} + S^{y2}) \tag{135}$$

Due the all-to-all nature of the effetive Hamiltonian one can find $K!$ possible relative arrangement of those K channels which keeps the Hamiltonian invariant. Here we briefly discuss the choice of the closed loop $\mathcal{C}_\mu$ and the insertion of the flux. As shown in the Fig.15(b) we have chosen a particular closed path which crosses all the outer spin only once. We embed that closed loop on a plane and put the flux perpendiculr to the plane through the closed loop. One can find a different closed loop where the ordering of the outer spins will be different. The action of the translation operator shifts the outer spins along this closed curve by one step.

The action of the twist operator on the S^x is determined in the follwoing calculation

Thus in the large channel limit

$$\begin{aligned}
&\lim_{K\to\infty} \hat{\mathcal{O}}_\mu H_{eff} \hat{\mathcal{O}}_\mu^\dagger \\
&= \frac{\beta_\uparrow(\alpha,\omega_\uparrow)}{2}\left[\hat{\mathcal{O}}_\mu S^x \hat{\mathcal{O}}_\mu^\dagger \hat{\mathcal{O}}_\mu S^x \hat{\mathcal{O}}_\mu^\dagger + \hat{\mathcal{O}}_\mu S^y \hat{\mathcal{O}}_\mu^\dagger \hat{\mathcal{O}}_\mu S^y \hat{\mathcal{O}}_\mu^\dagger\right] \\
&= \frac{\beta_\uparrow(\alpha,\omega_\uparrow)}{2}\left[S^{x2} + S^{y2}\right] = H_{eff} \\
&\lim_{K\to\infty} [\hat{\mathcal{O}}, H_{eff}] = 0
\end{aligned} \tag{136}$$

The translation operator $\hat{T}_\mu = e^{i\hat{\mathcal{P}}_\mu}$ commutes with the Hamiltonian thus the generator $\hat{\mathcal{P}}_\mu$ also commutes with the Hamiltonian. We can label the j^{th} state with the eigenvalues of this operator $\hat{\mathcal{P}}_\mu$ as $|p_\mu^j\rangle$. We here discuss the action of these twist and translation operators on these states.

$$\begin{aligned}
\hat{T}_\mu |p_\mu^j\rangle &= e^{i\hat{\mathcal{P}}_\mu}|p_\mu^j\rangle = e^{ip_\mu^j}|p_\mu^j\rangle \\
\hat{T}_\mu \hat{\mathcal{O}}_\mu |p_\mu^j\rangle &= \hat{\mathcal{O}}_\mu \hat{T}_\mu e^{i\frac{2\pi m}{K}}|p_\mu^j\rangle \quad , \\
&\qquad \text{here } m \text{ signifies different } S^z \text{ plateaux.} \\
&= \hat{\mathcal{O}}_\mu e^{i(\frac{2\pi m}{K} + p_\mu^j)}|p_\mu^j\rangle \ , \quad \frac{2\pi m}{K} \equiv p_\mu^m \\
\hat{T}_\mu\left(\hat{\mathcal{O}}_\mu|p_\mu^j\rangle\right) &= e^{i(p_\mu^m + p_\mu^j)}\left(\hat{\mathcal{O}}_\mu|p_\mu^j\rangle\right)
\end{aligned} \tag{137}$$

Thus we can see that $\hat{\mathcal{O}}_\mu|p_\mu^j\rangle$ is a state of the translation operator with different eigenvalue than $|p_\mu^j\rangle$, thus orthogonal to each other. Similarly one can generally show that $\langle p_\mu^j|\hat{\mathcal{O}}_\mu^q|p_\mu^j\rangle = 0$, where q is any integer. Also in the large K limit we can see from the eq.(136) that these different twisted states has same energy. Which shows that at each plateau state labeled by the S^z eigenvalue has K fold degenerate eigenstates labeled by the eigenvalue of the translation operators. Thus the CSCO is formed by $H, S^z, \hat{T}$. Thus states can be labeled as $|E, S_j^z, P_\mu^j\rangle$.

VI. TOPOLOGY AND GAUGE THEORY

A. In our case of stargraph model

In our model we find two string operators $\hat{\mathbb{Z}} = \sigma_d^z \Pi_{i=1}^K \sigma_i^z$ and $\hat{\mathbb{X}} = \sigma_d^x \Pi_{i=1}^K \sigma_i^x$, where K is the number of channels. These two operators commutes with the Hamiltonian H of this stargraph.

$$[H, \hat{\mathbb{Z}}] = 0 = [H, \hat{\mathbb{X}}] \tag{138}$$

We can rewrite the operators in the form of a twist operator as,

$$\mathbb{Z} = \sigma_d^z \prod_{i=1}^K \sigma_i^z = \frac{1}{i^{K+1}} e^{i\frac{\pi}{2}\sum_i \sigma_i^z} = e^{i\frac{\pi}{2}\sum_i(\sigma_i^z - 1)} = e^{i\pi\sum_i(S_i^z - 1/2)} \tag{139}$$

Similarly one can rewrite

$$\mathbb{X} = \sigma_d^x \prod_{i=1}^K \sigma_i^x = e^{i\pi\sum_i(S_i^x - 1/2)} \tag{140}$$

The commutation between these two operators are given as

$$[\mathbb{Z}, \mathbb{X}] = \prod_{i=d,1}^K \sigma_i^z \prod_{i=d,1}^K \sigma_i^x \left[1 - (-1)^{K+1}\right] \tag{141}$$

Thus we can see that for case where number of channels is odd that means $K+1$ is even, these two string operators commutes with each other forming a CSCO $(H, \hat{\mathbb{Z}}, \hat{\mathbb{X}})$. On the other hand in the case where number of channels K is even, these two operators does not commute with each other. Let's discuss these two cases seperately.

1. $K = odd$

In the case where the number of channels K is odd, we get $[\mathbb{Z}, \mathbb{X}] = 0$. Thus forming a CSCO with elements $H, \hat{\mathbb{Z}}, \hat{\mathbb{X}}$. Thus one can label the states using the eigenvalues of these operators. For the case of $K = 2n+1$ channels, the grounf state is K fold degenerate and labeled by the eigenvalues of the operator J^z which can take values $J^z = [-J, -J+1, \cdots, J-1, J]$, where $J = (K-1)/2$. For the odd channel case J^z can take zero value. Thus

$$|J^z\rangle \equiv |Z, X\rangle \tag{142}$$

where the eigenvalue Z can take $(K+1)/2$ values related to the absolute $|J^z|$ but cannot distinguish between $\pm J^z$ and X can take two values ± 1 which breaks the degenercy between $\pm J^z$. Thus these two operators together can uniquely label all the degenerate states.

B. Main

We can define two operators, for convenience let's call translation and twist operator respectively, $\hat{T}$ and $\hat{O}$ defined as

$$\hat{T} = e^{i\frac{2\pi}{K}\hat{\Sigma}} \ , \ \hat{O} = e^{i\hat{\phi}} \ , \ \ \hat{\Sigma} = [\hat{J}^z - (K-1)/2] \quad (143)$$

One can see that the generators of these above operators commutes with the Hamiltoninan, $[H, J^x] = [H, J^z] = [H, J^z] = 0$. In the large channel limit we can do semi-claassical approximation. As J^x and J^y both commutes with the Hamiltonian H then $[H, J^y(J^x)^{-1}] = 0$, and any non-singular function of these operators must also commute with the Hamiltonian, thus we can say that

$$\hat{\phi} = \tan^{-1}(\hat{J}^y(\hat{J}^x)^{-1}) \quad (144)$$

Then we get $[\hat{\phi}, \hat{H}] = 0$. We can label the ground states by the eigen values of the translation operator $\hat{T}$. We can also use the ground states labeled by the eigenvalues of J^z (M, say). Then the ground states are

$$|M_1\rangle, |M_2\rangle, |M_2\rangle, \cdots, |M_K\rangle \quad (145)$$

Then the operations of the translation operators on this states are give below.

$$\hat{T}|M_i\rangle = e^{i\frac{2\pi}{K}[M_i-(K-1)/2]}|M_i\rangle = e^{i2\pi\frac{p_i}{K}}|M_i\rangle \ , \ p_i \in [1, \cdots, K] \quad (146)$$

Now we check the braiding rule between the twist and the translation operators, we find

$$\begin{aligned} \hat{T}\hat{O}\hat{T}^\dagger\hat{O}^\dagger &= e^{\frac{2\pi}{K}[i\hat{\Sigma}, i\hat{\phi}]} = e^{i\frac{2\pi}{K}} \\ \hat{T}\hat{O}^m\hat{T}^\dagger\hat{O}^{\dagger m} &= e^{\frac{2\pi}{K}[i\hat{\Sigma}, im\hat{\phi}]} = e^{i2\pi\frac{m}{K}} \end{aligned} \quad (147)$$

Next we shown that the states $\hat{O}^m|M_i\rangle$ are orthogonal to each other and with the state $|M_i\rangle$.

$$\begin{aligned} \hat{T}\hat{O}^m|M_i\rangle &= \hat{O}^m\hat{T}e^{i2\pi\frac{m}{K}}|M_i\rangle = \hat{O}^m e^{i\frac{2\pi(m+p_i)}{K}}|M_i\rangle \\ \hat{T}\left(\hat{O}^m|M_i\rangle\right) &= e^{i\frac{2\pi(m+p_i)}{K}}\left(\hat{O}^m|M_i\rangle\right) \end{aligned} \quad (148)$$

Thus different states $\hat{O}^m|M_i\rangle$ for different m are labeled by different eigenvalues of the translation operations, thus are orthogonal to each other. Now as the twist operator $\hat{O}$ commutes with the Hamiltonian, thus we can see that

$$\langle M_i|\hat{O}^{m\dagger}H\hat{O}^m|M_i\rangle = \langle M_i|H|M_i\rangle \quad (149)$$

Thus the energy eigen values of all the orthogonal states are equal. Thus all the K mutually orthogonal states are degenerate.

VII. DUALITY IN THE MCK MODEL

We start from a strong coupling ($J \to \infty$) spin-S impurity MCK Hamiltonian in the over-screened regime ($K > 2S$),

$$H(J) = \sum_{k,\sigma,l} \epsilon_{k,l}\hat{n}_{k\sigma,l} + J\vec{S}_d \cdot \vec{s}_{\rm tot} \ . \quad (150)$$

Here, $\vec{s}_{\rm tot}$ is the total spin $\sum_l \sum_{kk'\alpha\beta} \vec{\sigma}_{\alpha\beta} c^\dagger_{k\alpha,l} c_{k'\beta,l}$ of all the zero modes. At strong-coupling, the ground states of the star graph eq. 8 act as a good starting point for a perturbative expansion. As argued previously, there are $K - 2S + 1$ ground states, labeled by the K values of the total spin angular momentum $S^z = S^z_d + s^z_{\rm tot} = -\frac{K}{2} + S, -\frac{K}{2} + S + 1, \ldots, \frac{K}{2} - S$. To leverage the large coupling, one can define a new spin impurity $\mathbb{S}$ out of this ground state manifold. Since the degeneracy of a spin is given by its multiplicity $2S' + 1$, we have $2S' + 1 = K - 2S + 1 \implies S' = \frac{K}{2} - S$. That is, the spin-$S$ impurity has a dual described by a spin-$(K - 2S + 1)$ impurity. The states of this new spin are defined by

$$\begin{aligned} \mathbb{S}^z_d|S^z\rangle &= S^z|S^z\rangle \, , \\ \mathbb{S}^\pm_d|S^z\rangle &= \sqrt{S'(S'+1) - S^z(S^z \pm 1)}|S^z \pm 1\rangle \end{aligned} \quad (151)$$

The excited states of the star graph can be used to define bosons [31], and the hopping into the lattice can then be re-written using these Bosons. One can then remove the single-particle hoping between the zero modes and the first sites using a Schrieffer-Wolff transformation in the small coupling $J' = \gamma\frac{4t^2}{J}$, and generate an exchange-coupling between the new impurity $\vec{\mathbb{S}}_d$ and the new zero modes formed out of the remaining sites in the lattice [31] (by remaining, we mean those real space sites that have not been consumed into forming the new spin). The new Hamiltonian, characterized by the small super-exchange coupling J', has the form

$$H'(J') = \sum_{k,\sigma,l} \epsilon_{k,l}\hat{n}_{k\sigma,l} + J'\vec{\mathbb{S}}_d \cdot \vec{s'}_{\rm tot} \quad (152)$$

The prime on $s_{\rm tot}$ indicates that it is formed by the new zero modes. This Hamiltonian is very similar to the one in eq. 150, and that is the essence of the strong-weak duality: One can go from the over-screened strong coupling spin-S MCK model to another over-screened weak coupling spin-$(K - 2S + 1)$ MCK model. For the case of $K = 4S$, we have $S' = S$, and both S_d and $\mathbb{S}_d$ describe the same spin objects (at least formally). The two models are then said to be self-dual. For example, for the case of spin-half MCK model, two-channel model is self-dual.

One important consequence of the duality relationship between the two over-screened models is that the RG equations are also dual; while the strong coupling model has an irrelevant coupling J that flows down to the intermediate fixed point J^*, the weak coupling model has

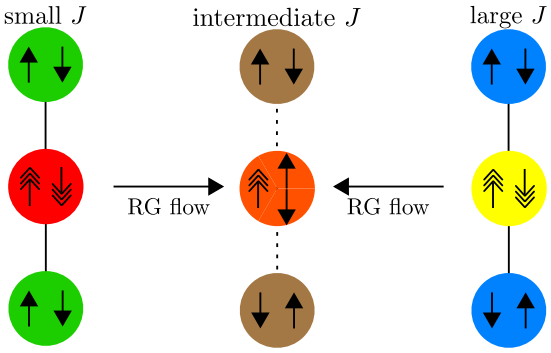

FIG. 16. Duality of the RG flows as seen in the star graph Hamiltonian. The red and green circles represent the impurity and zeroth site spins respectively. At large J, the red circle binds with the green circles to form an effective spin $\frac{K-1}{2}$ object (yellow) that interacts with the remaining spin of the conduction bath (blue circles).

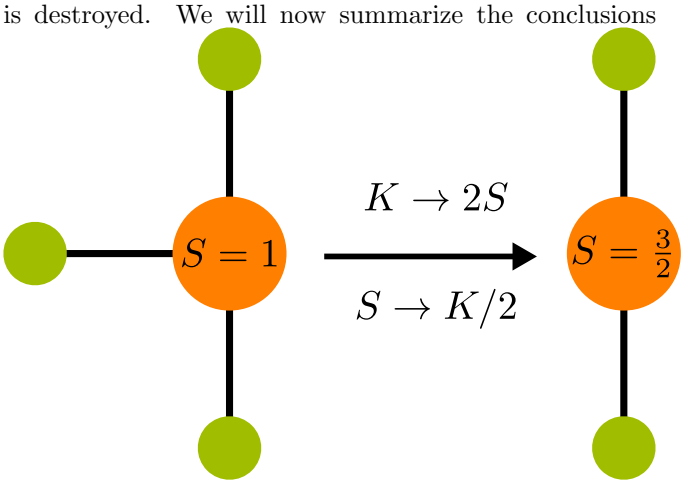

FIG. 17. ./duality2.pdf

a relevant coupling J' that flows up to the same fixed point $J'^* = J^*$. From the RG equation for the general spin-S MCK model, we know that $J'^* = \frac{2}{K\rho'}$, where ρ' is the DOS for the bath of the weak coupling Hamiltonian. This constrains the form of the scaling factor γ:

$$J'^* = \frac{\gamma 4t^2}{J^*} = \frac{2}{K\rho'} \implies \gamma = \frac{1}{4t^2}J^{*2} = \frac{1}{K^2t^2\rho\rho'} \quad (153)$$

There exists another set of dual points in the MCK model. This was hinted at when we looked at the degree of compassion in eq. 39. Since Γ depends only on the magnitude of δ, both $\pm\delta$ will give the same degree of compensation, same ground state energy and same ground state degeneracy $\left(g_K^S = |\delta| + 1\right)$. The definition of δ gives the duality transformation as $K \to 2S, S \to \frac{K}{2}$. That is, we transform from a $K-$channel MCK model with spin-S impurity, to a $2S$-channel MCK with a spin-$\frac{K}{2}$ impurity. The exactly-screened model $K = 2S$ maps on to itself and is therefore self-dual under this transformation.

For $K \neq 2S$, we transform an over-screened model into an under-screened model and vice versa. This duality relationship allows us to infer the RG scaling behaviour of one of the models if we know that of the other. If we know that for a certain pair of values K and S, the $K-$channel MCK model with spin-S impurity has an intermediate fixed point, we can immediately conclude that the $2S$-channel spin-$\frac{K}{2}$ model has a strong coupling fixed point.

VIII. IMPURITY QUANTUM PHASE TRANSITION IN THE MCK MODEL

A. RG phase diagram under anisotropy

The isotropic MCK mode undergoes a phase transition when the symmetry of the channel interaction strengths is destroyed. We will now summarize the conclusions of this section. It will be shown analytically that if, in a $K-$channel model, one of the couplings becomes slightly larger than the other $K-1$ couplings, the system goes into the singlet ground state characterized by local Fermi liquid excitations. On the other hand, if one of the couplings becomes slightly smaller than the rest, the system goes over to the $K-1$ channel Kondo model. *This shows that in the context of the general anisotropic MCK model, the symmetric model is highly unstable under slight anisotropy, and undergoes a phase transition into either the $K-1$ channel NFL phase or into the single channel LFL phase* (see fig. 19).

To see the transition, we need to start with the more general anisotropic MCK model:

$$H = \sum_{k,\alpha,l} \epsilon_{k,l}\hat{n}_{k\alpha,l} + \sum_{\substack{kk',\\ \alpha,\beta,l}} J_l \vec{S}_d \cdot \frac{1}{2}\vec{\sigma}_{\alpha\beta} c^\dagger_{k\alpha,l} c_{k'\beta,l} \ . \quad (154)$$

We now consider the specific case where $K-1$ channels have the same coupling $J_1 = J_2 = ... = J_{K-1} = J_+$ and the remaining channel has a different coupling $J_K = J_-$. The RG equations for such a model are

$$\frac{\Delta J_\pm}{|\Delta D|} = -\frac{J_\pm^2 \rho}{\mathcal{D}_\pm} + \frac{\rho^2 J_\pm}{2}\left[\frac{(K-1)J_+^2}{\mathcal{D}_+} + \frac{J_-^2}{\mathcal{D}_-}\right] \quad (155)$$

where $\mathcal{D}_\pm = \omega - \frac{D}{2} - \frac{J_\pm}{4}$ are the denominators of the URG equations. Setting $J_+ = J_-$ leads to the critical fixed point at $J_+^* = J_-^* = J_* = \frac{2}{K\rho}$. We now perturb around this fixed point by defining new variables $j_\pm = J_\pm - J_*$. We also assume that the bandwidth is large enough so that $\mathcal{D}_\pm \simeq \omega - \frac{D}{2} - \frac{J_*}{4} = -|\mathcal{D}_*|$. The RG equations then take the form

$$\frac{\Delta j_+}{|\Delta D|} = \frac{\rho J_+}{|\mathcal{D}_*|}\left[J_+ - \frac{\rho}{2}\left[(K-1)J_+^2 + J_-^2\right]\right] = \frac{\rho J_+}{KJ_*|\mathcal{D}_*|}\left[-(K-2)\,J_* j_+ - (K-1)j_+^2 - j_-^2 - 2J_* j_-\right] \quad (156)$$

$$\frac{\Delta j_-}{|\Delta D|} = \frac{J_-\rho}{|\mathcal{D}_*|}\left[J_- - \frac{\rho}{2}\left[(K-1)J_+^2 + J_-^2\right]\right] = \frac{J_-\rho}{KJ_*|\mathcal{D}_*|}\left[(K-2)\,J_* j_- - j_-^2 - (K-1)j_+^2 - 2(K-1)J_* j_+\right] \quad (157)$$

$$(158)$$

We will first look at the special case of $K = 2$, the two channel Kondo model. The equations simplify to

$$\frac{\Delta j_\pm}{|\Delta D|} = \frac{J_\pm \rho}{KJ_*|\mathcal{D}_*|}\left[-\left(j_+^2 + j_-^2\right) - 2J_* j_\mp\right] \quad (159)$$

For $j_- < 0, j_+ > 0$, we have $\Delta j_- < 0$. The coupling J_- therefore becomes irrelevant. For small j_+, we have $j_+^2 < 2J_*|j_-|$ and $\Delta j_+ > 0$. This means that the isotropic fixed point is repulsive under anisotropy [1]. The coupling j_+ being relevant means we have a single-channel Kondo problem. We already know the non-perturbative URG equation for the single-channel Kondo problem [8], and it leads to the strong coupling fixed point [1, 24, 58].

We now look at the general K channel case. Let us first look at the regime $j_- < 0, j_+ > 0$. In this regime, we have $\Delta j_- < 0$, which means j_- will flow to larger negative values until it reaches $j_- = -J_*$ such that $J_- = J_* + j_- = 0$. j_+ is, on the other hand, relevant for small values of $j_\pm$. It will continue to grow until the numerator of Δj_+ vanishes. This condition is given by

$$(K-2)\,J_* j_+ + (K-1)j_+^2 + j_-^2 + 2J_* j_- = 0 \quad (160)$$

Substituting $j_- = -J_*$ gives the fixed-point equation $(K-1)j_+^2 + (K-2)\,J_* j_+ - J_*^2 = 0$. Solving the equation gives

$$j_{+,*} = \frac{J_*}{2(K-1)}\left[-(K-2) \pm K\right] = \frac{J_*}{K-1} \quad (161)$$

At the final step, we chose the positive solution, because j_+ is relevant in this regime. The new fixed point value of J_+ is therefore

$$J_{+,*} = J_* + \frac{J_*}{K-1} = \frac{\frac{2}{K\rho}K}{K-1} = \frac{2}{(K-1)\rho} \quad (162)$$

In other words, the K channel fixed point flows to the $K-1$ channel fixed point. This is shown numerically in the left panel of fig. 18.

In the opposite regime $j_- > 0, j_+ < 0$, Δj_+ is negative. It has been checked numerically that J_+ ultimately flows to zero in this regime (middle and right panels of fig. 18), and J_- remains relevant. Since there is no numerator fixed point in the relevant coupling J_- and because all other couplings are irrelevant, the equation for J_- is replaced by the single-channel Kondo coupling URG equation, and the low-energy physics is then of strong coupling.

B. Robustness of the degeneracy in the presence of channel anisotropy

Here we start with the multi-channel zero mode model, any put anisotropy in the coupling α. Let's start with a simple possibility where there are two coupling α_1 and α_2, where both the α_1, α_2 are positive and negative. We write down the Hamiltonian corresponding to these cases,

$$H_{an} = \alpha_1 \vec{S}_d.\vec{S}_1 + \alpha_2 \vec{S}_d.\vec{S}_2 \quad (163)$$

There are K_1 and K_2 numbers of outer spins respectivelty which are connected to the central spin with the coupling with α_1 and α_2. Thus the total number of channels is $K = K_1 + K_2$. When $\alpha_1 = 0, \alpha_2 \neq 0$ then we end up with a multi-channel problem with K_1 number of channels thus the degeneracy becomes K_1 and for $\alpha_2 = 0, \alpha_1 \neq 0$ the degneracy becomes K_2. Though this can be trivially verified from the above Hamiltonian, the important property of this problem is the robustness of the ground state degeneracy. As we vary α_1 and α_2, to study the ground state degeneracy. We find that for any values α_1 and α_2 such that $\alpha_1/\alpha_2 \neq 0$ and $\alpha_2/\alpha_1 \neq 0$ the ground state degeneracy remains constant at $K = K_1 + K_2$. It is known in the literature [CITE someone] that under above mentioned anisotropy the low energy effective Hamiltonian becomes a multi-channel Kondo with smaller number of channels.

C. Berry phase

We start with the general multi-channel problem where the coupling strength with the central impurity spin of the i^{th} channel is α_i. Here our goal is to use the robustness of the ground state degeneracy of the star-graph model to build the gaue theoretic structure. We define the Hamiltonian of star-graph as

$$H_{st}(\vec{\alpha}) = \sum_{i=1}^{K} \alpha_i \vec{S}_d.\vec{S}_i \quad (164)$$

We define the K-dimensional soupling space where one possible sonfiguration is denoted by the vector $\vec{\alpha} = \mathcal{N}(\alpha_1, \alpha_2, \cdots, \alpha_K)$, where $\mathcal{N}$ is the normalization factor, where $\alpha_i \neq 0$ and $\alpha_i \neq \infty$, $\forall i \in [K]$. The Schrodinger equation for the Hamiltonian reads as

$$H_{st}(\vec{\alpha})\Psi_m(\vec{\alpha}) = E_m(\vec{\alpha})\Psi_m(\vec{\alpha}) \quad (165)$$

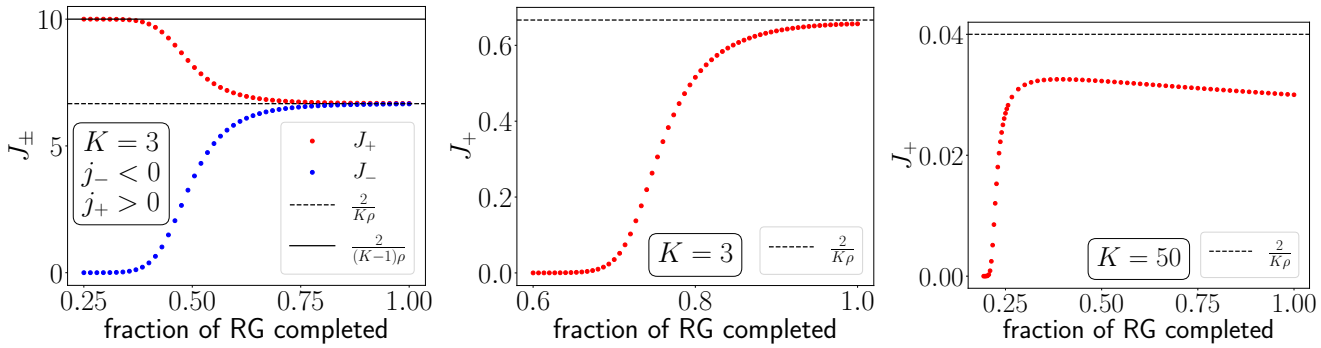

FIG. 18. left panel: Flow of $J_{\pm}$ when $j_{<}0$ and J_+. The smaller coupling J_- is irrelevant and switches off, while the other $K-1$ couplings J_+ flow to the $K-1$ MCK fixed point. Middle and right panels: Flow of the couplings J_+ when $j_+ < 0$ when $j_- > 0, j_+ < 0$, for two values of K. In both cases, the smaller coupling J_+ eventually dies out, leading to only one surviving coupling J^- which is relevant, and we are left with a single-channel Kondo model.

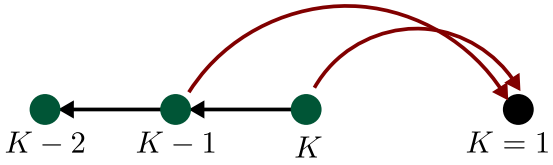

FIG. 19. Transitions from one Kondo model to another under insertion of anisotropy. The green circles represents MCK models with $K > 1$ while the black circle represents the $K = 1$ model. The red lines indicate transition from the K channel MCK model to the single-channel model when one of the exchange couplings becomes larger than the others. The black lines indicate the transition from the K channel model to the $K-1$ channel model when one of the exchange couplings becomes smaller than the others.

Here, we are only interested in the ground state manifold, where the energy of the state is E_g. Due to the degeneracy (K-fold) there are K states in that manifold with the same energy labeled by say k. Thus the equation for the ground state manifold reads

$$H_{st}(\vec{\alpha})\Psi_g^k(\vec{\alpha}) = E_g(\vec{\alpha})\Psi_g^k(\vec{\alpha}) \tag{166}$$

One can do a simple transformation to make the ground state energy zero. Thus

$$\begin{aligned} H_{st}(\vec{\alpha})\Psi_g^k(\vec{\alpha}) &= 0 \\ i\hbar\frac{\partial\Psi(\alpha(\vec{t}))}{\partial t} &= H_{st}(\alpha(\vec{t}))\Psi(\alpha(\vec{t})) = 0 \end{aligned} \tag{167}$$

As the ground state is degenerate one can take any linera combinations of the states to create arbitrary basis state (orthogonal and normalized). Let's say $\psi_k(\vec{\alpha}(t))$ represents the arbitrary basis state, which should be smooth in t locally and follow the Schrodinger equation,

$$H_{st}(\vec{\alpha}(t))\psi_k(\vec{\alpha}(t)) = 0 \tag{168}$$

We here try to find the solution of the Eq.(167), we start with the trial solution

$$\eta_a(t) = U_{ab}(t)\psi_b(t) \tag{169}$$

IX. CONCLUSIONS

In the URG analysis of the one dimensional Hubbard model [7], a study of the zero mode Hamiltonian (in that case, the Fermi surface itself) was sufficient to topologically characterize various phases of the Berezinskii-Kosterlitz-Thouless (BKT) RG phase diagram.

ACKNOWLEDGMENTS

The authors thank P. Majumdar, A. Mitchell, S. Sen, S. Patra, M. Mahankali and R. K. Singh for several discussions and feedback. Anirban Mukherjee thanks the CSIR, Govt. of India and IISER Kolkata for funding through a research fellowship. Abhirup Mukherjee thanks IISER Kolkata for funding through a research fellowship. AM and SL thank JNCASR, Bangalore for hospitality at the inception of this work. NSV acknowledges funding from JNCASR and a SERB grant (EMR/2017/005398).

Appendix A: Hamiltonian RG of spin-S impurity MCK Model

The Hamiltonian for the channel-isotropic MCK model is given in eq. II A. As mentioned in the same section, the Hamiltonian $H_{(j-1)}$ of the $(j-1)^{\text{th}}$ RG step is obtained from the Hamiltonian $H_{(j)}$ of the preceding RG step by applying a unitary transformation $U_{(j)}$: $H_{(j-1)} = U_{(j)}H_{(j)}U_{(j)}^\dagger$. The unitary transformation is obtained in terms of the fermionic operator $\eta_{(j)}$:

$$U_{(j)} = \frac{1}{\sqrt{2}}\left(1 + \eta_{(j)} - \eta_{(j)}^\dagger\right) , \tag{A1}$$

$$\hat{\omega}_{(j)} = H_{(j-1)} - H_{(j)}^i,\ T_{(j)} \equiv \mathrm{Tr}\left(H_{(j)}c_j\right) , \tag{A2}$$

$$\eta_{(j)}^\dagger = \frac{1}{\hat{\omega}_{(j)} - \mathrm{Tr}\left(H_{(j)}\hat{n}_j\right)}c_j^\dagger T_{(j)} . \tag{A3}$$

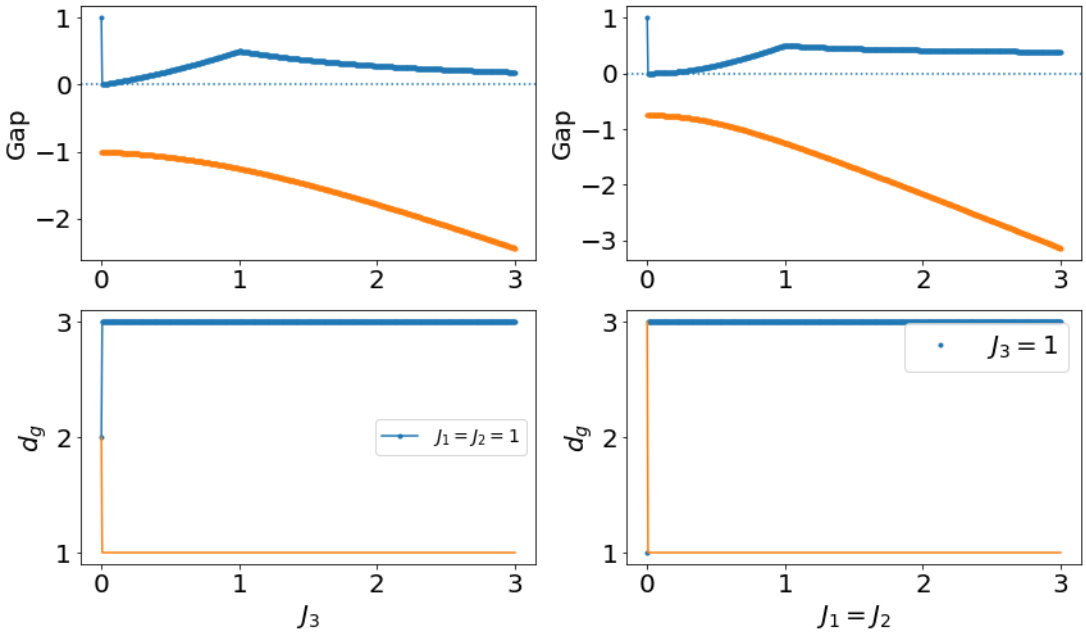

FIG. 20. Add proper figures.

The operator $\hat{\omega}_{(j)}$ encodes the quantum fluctuation scales arising from the interplay of the kinetic energy terms and the interaction terms of the Hamiltonian.

The URG equation for the single-channel Kondo model [8] shows a stable strong-coupling fixed point. Ferromagnetic interactions are irrelevant. Strictly speaking, that RG equation already encodes, in principle, the multi-channel behaviour, through a modified $\hat{\omega}$. To extract this information, we consider the strong-coupling fixed-point $J \gg D$ as a fixed point and analyze its stability from the star graph perspective. For the exactly-screened case, the star graph decouples from the conduction bath, leaving behind a local Fermi liquid interaction on the first site. Similarly, in the under-screened regime, the ground state is composed of states where the impurity spin is only partially screened by the conduction channels. If a particular configuration of the bath-impurity system has the total conduction bath spin down, the impurity will have a residual up spin. This induces a ferromagnetic super-exchange coupling that is irrelevant under RG, so this fixed point is stable as well.

We now come to the over-screened case, where there is a residual spin on the conduction channel site. The neighbouring electrons will now hop in with spins opposite to that of the impurity, so an antiferromagnetic interaction will be induced, and such an interaction is relevant under the RG. This shows that the over-screened regime cannot have a stable strong-coupling fixed point, and we need to search for an intermediate coupling fixed point. We therefore need the generator of the unitary transformation that incorporates third order scattering scatterings explicitly. We should take account of all possible processes that render the set of states $\{|\hat{n}_{q\beta} = 1\rangle, |\hat{n}_{q\beta} = 0\rangle\}$ diagonal. The higher order generator itself has two scattering processes, such that the entire renormalisation term $c^\dagger_{q\beta} T\eta$ has in total three coherent processes. The complete generator upto third order can be written as

$$\eta = \frac{1}{\hat{\omega} - H_D} T^\dagger c \simeq \frac{1}{\omega' - H_D} T^\dagger c + \frac{1}{\omega' - H_D} H_X \frac{1}{\omega' - H_D} T^\dagger c + \frac{1}{\omega' - H_D} T^\dagger c \frac{1}{\omega' - H_D} H_X \tag{A4}$$

where $H_X = J \sum_{k,k'<\Lambda_j,\alpha,\alpha'} \vec{S}_d \cdot \vec{s}_{\alpha\alpha'} c^\dagger_{k\alpha} c_{k'\alpha'}$ is scattering between the entangled electrons. There are two third order terms in the above equation corresponding to the two possible sequences in which the processes can occur while keeping the total renormalisation $c^\dagger_{q\beta} T\eta$ diagonal in $q\beta$. The second order processes remain unchanged. The total renormalisation takes the form:

$$\Delta H_{(j)} = \underbrace{c^\dagger T \frac{1}{\omega' - H_D} T^\dagger c + \left(c^\dagger \leftrightarrow c\right)}_{\Delta H^{(2)}_{(j)}} + \underbrace{c^\dagger T \frac{1}{\omega' - H_D} H_X \frac{1}{\omega' - H_D} T^\dagger c + c^\dagger T \frac{1}{\omega' - H_D} T^\dagger c \frac{1}{\omega' - H_D} H_X + \left(c^\dagger \leftrightarrow c\right)}_{\Delta H^{(3)}_{(j)}} \tag{A5}$$

$\Delta H^{(2)}_{(j)}$ and $\Delta H^{(3)}_{(j)}$ are the renormalisation arising from the the second and third order processes respectively.

It is easier to see the RG flow of the couplings if we write the Hamiltonian in terms of the eigenstates of S^z_d. These eigenstates are defined by $S^z_d |m_d\rangle = m_d |m_d\rangle, m_d \in [-S, S]$. In terms of these eigenstates, the Hamiltonian becomes

$$\mathcal{H} = \sum_{k\sigma} \epsilon_k \tau_{k\sigma} + \sum_{m_d=-S}^{S} \sum_{\substack{kl,\\ \sigma=\uparrow,\downarrow}} J^{\sigma}_{m_d} |m_d\rangle \langle m_d| c^{\dagger}_{k\sigma} c_{l\sigma} + \sum_{kl} \sum_{m_d=-S}^{S-1} J^{t}_{m_d} \left(|m_d+1\rangle \langle m_d| s^{-}_{kl} + \text{h.c.} \right) \tag{A6}$$

where k, l sum over the momentum states, σ sums over the spin indices, $J^{\sigma}_m = \frac{1}{2}\sigma m J$ in the UV Hamiltonian, and $J^t_m = J\frac{1}{2}\sqrt{S(S+1) - m(m+1)}$ is the coupling that connects $|m\rangle$ and $|m+1\rangle$. We first calculate $\Delta H^{(2)}_{(j)}$. There will be two types of processes - those processes that start from an occupied state (particle sector) and those that start from a vacant state (hole sector). Due to particle hole symmetry of the Hamiltonian, they will be equal to each other and we will only calculate the particle sector contribution.

In the particle sector, we have ($\hat{n}_{q\beta} = 1$), so we will work at a negative energy shell $\epsilon_q = -D$. The renormalisation can schematically represented as $H^I_0 \frac{1}{\omega - H^D_{q\beta}} H^I_1$. Both H^I_0 and H^I_1 have all three operators $S^z_d, S^{\pm}_d$. We first consider specifically the case of spin-$\frac{1}{2}$ impurity. Those terms that have identical operators on both sides can be ignored because ${S^z_d}^2 =$ constant and ${S^{\pm}}^2 = 0$. All the six terms that *will* renormalise the Hamiltonian have a spin flip operator on at least one side of the Greens function. This means that in the denominator of the Greens function, S^z_d and s^z_{qq} have to be anti-parallel in order to produce a non-zero result for that term. This means we can identically replace $S^z_d s^z_{qq} = -\frac{1}{4}$. Also, in the particle sector, the Greens function always has $c_{q\beta}$ in front of it, so $\epsilon_q \tau_{q\beta} = \frac{D}{2}$. The upshot of all this is that the denominator of all scattering processes for the spin-$\frac{1}{2}$ impurity Hamiltonian will be $\omega - \frac{D}{2} + \frac{J}{4}$.

We now come to the general case of spin-S impurity. The various terms that renormalise the Hamiltonian can be described in terms of the bath spin operators that come into them. For example, the term that has s^z on both sides of the intervening Greens function can be represented as $z|z$. There are 7 such terms: $z|z, \pm|\mp, z|\pm, \pm|z$. Each of these terms occur both in the particle and the hole sectors. We will demonstrate the calculation of two of these terms. The $z|z$ $+|-$ terms evaluate in the following manner.

$$z|z : \sum_{kk',m,\sigma} c^{\dagger}_{q\sigma} c_{k'\sigma} |m\rangle \langle m| \frac{{J^{\sigma}_m}^2}{\omega - \frac{D}{2} + \frac{J}{2}\sigma S^z_d} |m\rangle \langle m| c^{\dagger}_{k\sigma} c_{q\sigma} = -\sum_{kk',m,\sigma} n_{q\sigma} \frac{{J^{\sigma}_m}^2 c^{\dagger}_{k\sigma} c_{k'\sigma} |m\rangle \langle m|}{\omega_{m,\sigma} - \frac{D}{2} + \frac{J}{2}\sigma m} \tag{A7}$$

$$+|- : \sum_{kk',m} c^{\dagger}_{q\uparrow} c_{k'\downarrow} |m\rangle \langle m+1| \frac{{J^t_m}^2}{\omega - \frac{D}{2} + \frac{J}{2} S^z_d} |m+1\rangle \langle m| c^{\dagger}_{k\downarrow} c_{q\uparrow} = -n_{q\uparrow} \sum_{kk',m} \frac{{J^t_m}^2 c^{\dagger}_{k\downarrow} c_{k'\downarrow} |m\rangle \langle m|}{\omega_{m+1,\uparrow} - \frac{D}{2} + \frac{J}{2}(m+1)} \tag{A8}$$

We similarly compute the rest of the terms. We again define $\sum_q \hat{n}_{q\sigma} = n(D)$. To compare with the spin-$\frac{1}{2}$ RG equations, we will transform the general spin-S ω to the spin-$\frac{1}{2}$ ω, using $\omega_{m,\sigma} \to \omega - \frac{J}{2}\left(m\sigma - \frac{1}{2}\right)$.

The renormalisation in J^{σ}_m is

$$\Delta J^{\sigma}_m = -n(D) \frac{\left(J^{\sigma}_m\right)^2 + \left(J^t_{m-\frac{1+\sigma}{2}}\right)^2}{\omega - \frac{D}{2} + \frac{J}{4}} \,. \tag{A9}$$

Here, we have defined $J^t_m = 0$ for $|m| > S$. Two relations can be obtained from this RG equation, the RG equations for the sum and difference of the couplings: $J^{\pm}_m = \frac{1}{2}\left(J^{\uparrow}_m \pm J^{\downarrow}_m\right)$. The RG equation for the sum of the couplings is

$$\begin{aligned} \Delta J^{+}_m &= -n(D) \frac{\sum_{\sigma} \left(J^{\sigma}_m\right)^2 + \sum_{\sigma} \left(J^t_{m-\frac{1+\sigma}{2}}\right)^2}{2\left(\omega - \frac{D}{2} + \frac{J}{4}\right)} \\ &= -n(D) \frac{J^2}{4} \frac{S(S+1)}{\omega - \frac{D}{2} + \frac{J}{4}} \end{aligned} \tag{A10}$$

This is an $m-$independent piece, so it can be summed over to produce an impurity-independent potential scattering term, which we ignore.

The second is the RG equation for the difference of the couplings:

$$\Delta J^{-}_m = -n(D) \frac{1}{2} \frac{\left(J^t_{m-1}\right)^2 - \left(J^t_m\right)^2}{\omega - \frac{D}{2} + \frac{J}{4}} = -\frac{1}{4} \frac{n(D) m J^2}{\omega - \frac{D}{2} + \frac{J}{4}} \tag{A11}$$

The usual J Kondo coupling is recovered through $J = 2J_m^-/m$. Substituting this gives

$$\Delta_{\text{p sector}} J = -\frac{1}{2} n(D) \frac{J^2}{\omega - \frac{D}{2} + \frac{J}{4}} \tag{A12}$$

We can also obtain the RG equation for J from the transverse renormalisation:

$$\Delta J_m^t = -\frac{n(D) J_m^t \left(J_m^\downarrow + J_{m+1}^\uparrow \right)}{\omega - \frac{D}{2} + \frac{J}{4}} = -\frac{1}{2} \frac{n(D) J_m^t J}{\omega - \frac{D}{2} + \frac{J}{4}} \tag{A13}$$

Since $J_m^t \propto J$, we have

$$\Delta J_{\text{p sector}} = -\frac{1}{2} \frac{n(D) J^2}{\omega - \frac{D}{2} + \frac{J}{4}} \tag{A14}$$

The total renormalisation from both particle and hole sectors, at this order, is

$$\Delta J^{(2)} = -\frac{n(D) J^2}{\omega - \frac{D}{2} + \frac{J}{4}} \tag{A15}$$

We now come to the third order renormalisation. Following eq. A5, the next order renormalisation is

$$\begin{aligned} \Delta H_j^{(3)} = c^\dagger T \frac{1}{\omega' - H_D} H_X \frac{1}{\omega' - H_D} T^\dagger c \\ + c^\dagger T \frac{1}{\omega' - H_D} T^\dagger c \frac{1}{\omega' - H_D} H_X \end{aligned} \tag{A16}$$

The first term will be of the form

$$\sum_{q,k,l_1} c^\dagger_{q\beta,l_1} c_{k\alpha,l_1} \left|m_1\right\rangle \left\langle m_2\right| \frac{1}{\omega - \frac{D}{2} - \frac{\epsilon_k}{2} + \frac{\beta J}{4} S_d^z} \left|m_2\right\rangle c^\dagger_{k_1\sigma_1,l_2} c_{k_2\sigma_2,l_2} \left\langle m_3\right| \frac{1}{\omega - \frac{D}{2} - \frac{\epsilon_k}{2} + \frac{\beta J}{4} S_d^z} \left|m_3\right\rangle \left\langle m_4\right| c^\dagger_{k\alpha,l_1} c_{q\beta,l_1} \tag{A17}$$

We have not bothered to write all the summations and the couplings correctly, because we will only simplify the denominator here. Evaluating the inner products gives

$$\sum_{qk,l_1} \frac{\left|m_1\right\rangle \left\langle m_4\right| c^\dagger_{q\beta} c_{k\alpha} c^\dagger_{k_1\sigma_1,l_2}}{\omega_{m_2,\beta} - \frac{D}{2} - \frac{\epsilon_k}{2} + \frac{\beta J m_2}{4}} \frac{c_{k_2\sigma_2,l_2} c^\dagger_{k\alpha} c_{q\beta}}{\omega_{m_3,\beta} - \frac{D}{2} - \frac{\epsilon_k}{2} + \frac{\beta J m_3}{4}} \tag{A18}$$

We again use $\omega_{m,\sigma} \to \omega - \frac{J}{2}\left(m\sigma - \frac{1}{2}\right)$.

$$\left|m_1\right\rangle \left\langle m_4\right| c^\dagger_{k_1\sigma_1,l_2} c_{k_2\sigma_2,l_2} \sum_{qk,l_1} \frac{\hat{n}_{q\beta}\left(1 - \hat{n}_{k\alpha}\right)}{\left(\omega - \frac{D}{2} - \frac{\epsilon_k}{2} + \frac{J}{4}\right)^2} \tag{A19}$$

We define $\sum_q \hat{n}_{q\beta} = n(D)$. Performing the sums over k and l_1 gives

$$-\frac{1}{2} \left|m_1\right\rangle \left\langle m_4\right| c^\dagger_{k_1\sigma_1,l_2} c_{k_2\sigma_2,l_2} \frac{\rho n(D) K}{\omega - \frac{D}{2} + \frac{J}{4}} \tag{A20}$$

ρ is the density of states which we have taken to be constant. Reinstating the complete summation and the couplings gives

$$-\frac{1}{2} \frac{\rho n(D) K}{\omega - \frac{D}{2} + \frac{J}{4}} \sum_{\substack{m_1,m_4,k_1,k_2,\\ l_2,\sigma_1\sigma_2}} \lambda_1\lambda_2\lambda_3 \left|m_1\right\rangle \left\langle m_4\right| c^\dagger_{k_1\sigma_1,l_2} c_{k_2\sigma_2,l_2} \tag{A21}$$

There is no sum over m_2 and m_3 because they are constrained by m_1 and m_4 respectively. λ_i represent the couplings present at the three interaction vertices. $k_{1,2}$ sum over the momenta, $\sigma_{1,2}$ sum over the spin indices and l_2 sums over the channels.

The second term in eq. A16 can be evaluated in an almost identical fashion. The integral here be negative of the first term, because of an exchange in the scattering processes.

$$\frac{1}{2} \frac{\rho n(D) K}{\omega - \frac{D}{2} + \frac{J}{4}} \sum_{\substack{m_1,m_4,k_1,k_2,\\ l_2,\sigma_1\sigma_2}} \lambda_1\lambda_3\lambda_2 \left|m_1\right\rangle \left\langle m_4\right| c^\dagger_{k_1\sigma_1,l_2} c_{k_2\sigma_2,l_2} \tag{A22}$$

The first group of terms (those that appear in A21) in the particle sector can be represented as $a|b'|c$, where $a, b, c \in \{z, +, -\}$ and represent the operator for the conduction electrons in the three ceonnected processes. The $'$ on b indicates that it is the state of the electrons *not being decoupled*. The second group of terms (those that appear in A22) are therefore represented as $a|b|c'$, because in this group, the interaction H_X between the electrons that are not being decoupled occur at the very end. We will only calculate the terms in the particle sector, the ones in hole sector will be equal to these because of particle-hole symmetry. The full list of terms is: $z|z'|z$ $z|z|z'$ $-|z'|+$ $-|+|z'$ $+|z'|-$ $+|-|z'$ $z|+'|z$ $z|-'|z$ $+|+'|-$ $-|+'|+$ $z|z|+'$ $z|z|-'$ $+|-|+'$ $+|-|-'$ $-|+|+'$ $z|z'|z$ $z|z|z'$ $-|z'|+$ $-|+|z'$ $+|z'|-$ $+|-|z'$ $z|+'|z$ $z|-'|z$ $+|+'|-$ $-|+'|+$ $z|z|+'$ $z|z|-'$ $+|-|+'$ $+|-|-'$ $-|+|+'$.

The total renormalisation in J_m^σ is

$$\Delta J_m^\sigma = \frac{1}{2} \frac{\rho n(D) K}{\omega - \frac{D}{2} + \frac{J}{4}} \left[\left(J_{m-1}^t\right)^2 J_m^\sigma + \left(J_m^t\right)^2 J_m^\sigma - \left(J_{m-1}^t\right)^2 J_{m-1}^\sigma - \left(J_m^t\right)^2 J_{m+1}^\sigma \right] = \frac{1}{2} \frac{\rho n(D) K}{\omega - \frac{D}{2} + \frac{J}{4}} J^3 m\sigma \tag{A23}$$

Since we had defined $J^\sigma_m \equiv \frac{1}{2}Jm\sigma$, we have $\Delta J = \frac{2}{m\sigma}\Delta J^\sigma_m$, and we get $\Delta_{\text{p sector}} J = \frac{1}{4}\frac{\rho n(D)K}{\omega - \frac{D}{2} + \frac{J}{4}}J^3$. Combining with the hole sector renormalisation, we get

$$\Delta J^{(3)} = \frac{1}{2}\frac{\rho n(D)K}{\omega - \frac{D}{2} + \frac{J}{4}}J^3 \tag{A24}$$

The total renormalisation in J after combining all orders is

$$\Delta J = -\frac{n(D)J^2}{\omega - \frac{D}{2} + \frac{J}{4}} + \frac{1}{2}\frac{\rho n(D)K}{\omega - \frac{D}{2} + \frac{J}{4}}J^3 \tag{A25}$$

[1] Nozières, Ph. and Blandin, A., J. Phys. France **41**, 193 (1980).
[2] A. Mukherjee and S. Lal, New Journal of Physics **22**, 063008 (2020).
[3] A. Mukherjee and S. Lal, Nuclear Physics B **960**, 115170 (2020).
[4] A. Mukherjee and S. Lal, Nuclear Physics B **960**, 115163 (2020).
[5] S. Patra and S. Lal, Phys. Rev. B **104**, 144514 (2021).
[6] S. Pal, A. Mukherjee, and S. Lal, **21**, 023019 (2019).
[7] S. P. Anirban Mukherjee and S. Lal, Journal of High Energy Physics **2021** (2021), 10.1007/JHEP04(2021)148.
[8] A. Mukherjee, A. Mukherjee, N. S. Vidhyadhiraja, A. Taraphder, and S. Lal, (2021), arXiv:2111.10580 [cond-mat.str-el].
[9] J. Gan, **6**, 4547 (1994).
[10] E. Kogan, Journal of Physics Communications **2**, 085001 (2018).
[11] Y. Kuramoto, The European Physical Journal B - Condensed Matter and Complex Systems **5**, 457 (1998).
[12] A. M. Tsvelick and P. B. Wiegmann, Zeitschrift für Physik B Condensed Matter **54**, 201 (1984).
[13] N. Andrei and C. Destri, Phys. Rev. Lett. **52**, 364 (1984).
[14] G. Zaránd, T. Costi, A. Jerez, and N. Andrei, Phys. Rev. B **65**, 134416 (2002).
[15] N. Andrei and A. Jerez, Phys. Rev. Lett. **74**, 4507 (1995).
[16] A. M. Tsvelick, Journal of Physics C: Solid State Physics **18**, 159 (1985).
[17] A. M. Tsvelick and P. B. Wiegmann, Zeitschrift für Physik B Condensed Matter **54**, 201 (1984).
[18] I. Affleck and A. W. Ludwig, Nuclear Physics B **360**, 641 (1991).
[19] I. Affleck and A. W. Ludwig, Physical Review B **48**, 7297 (1993).
[20] A. W. W. Ludwig and I. Affleck, Phys. Rev. Lett. **67**, 3160 (1991).
[21] V. J. Emery and S. Kivelson, Phys. Rev. B **46**, 10812 (1992).
[22] J. von Delft, G. Zaránd, and M. Fabrizio, Phys. Rev. Lett. **81**, 196 (1998).
[23] H. B. Pang and D. L. Cox, Phys. Rev. B **44**, 9454 (1991).
[24] A. K. Mitchell, M. R. Galpin, S. Wilson-Fletcher, D. E. Logan, and R. Bulla, Phys. Rev. B **89**, 121105 (2014).
[25] V. Tripathi, Landau Fermi Liquids and Beyond (CRC Press, 2018).
[26] E. Fradkin, Field theories of condensed matter physics (Cambridge University Press, 2013).
[27] C. M. Varma and Y. Yafet, Phys. Rev. B **13**, 2950 (1976).
[28] K. Yosida, Phys. Rev. **147**, 223 (1966).
[29] K. G. Wilson, Reviews of Modern Physics **47**, 773 (1975).
[30] C. P. Moca, I. Weymann, M. A. Werner, and G. Zaránd, Phys. Rev. Lett. **127**, 186804 (2021).
[31] C. Kolf and J. Kroha, Phys. Rev. B **75**, 045129 (2007).
[32] R. Žitko and M. Fabrizio, Phys. Rev. B **95**, 085121 (2017).
[33] J. Gan, N. Andrei, and P. Coleman, Phys. Rev. Lett. **70**, 686 (1993).
[34] A. M. Tsvelick and P. B. Wiegmann, Journal of Statistical Physics **38**, 125 (1985).
[35] O. Parcollet and A. Georges, Phys. Rev. Lett. **79**, 4665 (1997).
[36] T. Kimura and S. Ozaki, Journal of the Physical Society of Japan **86**, 084703 (2017), https://doi.org/10.7566/JPSJ.86.084703.
[37] D. Bensimon, A. Jerez, and M. Lavagna, Phys. Rev. B **73**, 224445 (2006).
[38] D. L. Cox and M. Jarrell, **8**, 9825 (1996).
[39] P. Coleman, L. B. Ioffe, and A. M. Tsvelik, Phys. Rev. B **52**, 6611 (1995).
[40] P. Coleman and C. Pépin, Phys. Rev. B **68**, 220405 (2003).
[41] N. Roch, S. Florens, T. A. Costi, W. Wernsdorfer, and F. Balestro, Phys. Rev. Lett. **103**, 197202 (2009).
[42] A. Schiller and L. De Leo, Phys. Rev. B **77**, 075114 (2008).
[43] P. Durganandini, EPL (Europhysics Letters) **95**, 47003 (2011).
[44] K. G. Wilson, Rev. Mod. Phys. **47**, 773 (1975).
[45] P. Nozieres, Journal of Low Temperature Physics **17**, 31 (1974).
[46] N. Andrei, K. Furuya, and J. H. Lowenstein, Rev. Mod. Phys. **55**, 331 (1983).
[47] A. M. Tsvelick and P. B. Wiegmann, Adv. in Phys. **32**, 453 (1983).
[48] M. Vojta, Philosophical Magazine **86**, 1807 (2006), https://doi.org/10.1080/14786430500070396.
[49] A. K. Mitchell, M. Becker, and R. Bulla, Phys. Rev. B **84**, 115120 (2011).
[50] R. Bulla, T. Costi, and T. Pruschke, Rev. Mod. Phys. **80**, 395 (2008).
[51] V. Marić, S. M. Giampaolo, and F. Franchini, Communications Physics **3**, 220 (2020).

[52] A. C. Hewson, The Kondo Problem to Heavy Fermions (Cambridge University Press, 1993).
[53] C. Varma, Z. Nussinov, and W. Van Saarloos, Physics Reports **361**, 267 (2002).
[54] A. Mukherjee and S. Lal, New Journal of Physics **22**, 063007 (2020).
[55] P. W. Anderson, Phys. Rev. Lett. **18**, 1049 (1967).
[56] K. Yamada and K. Yosida, Progress of Theoretical Physics **59**, 1061 (1978), https://academic.oup.com/ptp/article-pdf/59/4/1061/5315849/59-4-1061.pdf.
[57] K. Yamada and K. Yosida, Progress of Theoretical Physics **62**, 363 (1979).
[58] M. Fabrizio, A. O. Gogolin, and P. Nozières, Phys. Rev. Lett. **74**, 4503 (1995).